



***COLLEGE OF SCIENCE AND TECHNOLOGY***



## **FINAL YEAR PROJECT REPORT:**

**A Numerical investigation into the effect of blade wrap angle on Splitter-Bladed Reversible Pump Turbines operating within the S-Shape Zone.**

**BY**

**Kunde Jean Claude**

**221030489**

**Supervisor: Dr. Maxime BINAMA**

**Academic Year: 2024 – 2025**

# DECLARATION

This project is the result of my original research conducted by **Kunde Jean Claude** (student number 221030489). It has not been submitted for any degree or qualification previously. All sources used in this work are properly cited and acknowledged.

Student Id	Names	Signature
1. 221030489	<b>Kunde Jean Claude</b>	.....

Approved by the supervisor: Dr. Maxime BINAMA

Signature.....

date: ... /.../.....

## **ABSTRACT**

This project investigates the impact of blade wrap angle on Splitter-Bladed on the flow and pressure field characteristics within a reversible pump turbine (RPT) using numerical simulations. RPTs are crucial in hydroelectric power generation due to their ability to operate in pumping, generating, and idle modes. The study aims to enhance the understanding of fluid dynamics in RPTs, focusing on how splitter blades and wrap angle can mitigate flow instabilities that lead to performance degradation, increased vibration, and mechanical wear.

The research explores various wrap angle configurations and their effects on flow patterns and pressure distribution. Using computational fluid dynamics (CFD), the study identified optimal blade wrap angle on Splitter-Bladed Reversible Pump Turbines to minimize flow instability across operating points. For instance, blade wrap angle WA1 proved most effective at OP8, while a different blade wrap angle, WA2, minimized instability at OP 9. We found significant variations in flow patterns and pressure pulsations depending on operating conditions. Introducing splitter blades significantly reduced these instabilities.

# Table of contents

DECLARATION .....	1
ABSTRACT.....	2
Acronyms .....	7
NOTATIONS.....	7
Chapter1 INTRODUCTION.....	9
1.1 Background .....	9
1.2 Problem statement.....	10
1.3 Main objective .....	11
1.4 Specific objective of this research include: .....	11
1.5 Research questions:.....	12
1.6 Justification .....	12
1.7 Scope.....	12
1.8 Report outline.....	13
Chapter2 LITERATURE REVIEW.....	14
2.1 Basic concept .....	14
2.1.1 History of A Reversible Pump Turbine .....	14
2.1.2 Reversible pump Turbine components .....	16
2.1.3 Classifications of Reversible pump Turbine.....	17
2.1.4 Reversible Pumps application.....	18
2.1.5 Pump operating conditions. ....	18
2.2 Similar works .....	19
2.2.1 Pump-Turbine Performance Improvement .....	19
2.2.2 Flow Behavior and Instability in Pump-Turbines.....	21
2.2.3 Pump-Turbine Stability and Pressure Pulsations .....	23
2.2.4 Pump-Turbine Operation and Design .....	24
2.3 Summary of previous works and their Gaps .....	25
2.3.1 Influence of Operating Conditions and Design: .....	25
2.3.2 Pressure Fluctuations and Turbine Stability .....	27
2.4 Chapter conclusion.....	28
Chapter3 METHODOLOGY.....	29
3.1 Previous methods.....	29

3.1.1 Experimental methods .....	29
3.1.2 Numerical methods .....	31
3.2 Methodology used.....	34
3.3 RPT Operation in Turbine Mode: .....	36
3.3.1 Mesh Generation:.....	36
3.3.2 Numerical scheme.....	37
Chapter4 RESULT DISCUSSION .....	40
4.1 Velocity streamlines characteristics and analysis .....	40
4.2 Pressure pulsation characteristics and analysis.....	48
Chapter5 Conclusion.....	63
Chapter6 Recommendations .....	65
References .....	66

## List of figures and tables

FIGURE 2-1 FIGURE 1 REVERSIBLE PUMP TURBINE COMPONENTS [9] .....	17
FIGURE 2-2 THE CONTOURS OF ENTROPY GENERATION RATE DISTRIBUTION AT MID SPAN FOR BOTH SCHEMES. [10] .....	20
FIGURE 2-3: STREAMLINES ON THE THREE SPANWISE SECTIONS WHEN THE BFVSS OCCUR ON THE HUB SIDE (15° GVO). (A) SECTION ON THE HUB SIDE, (B) SECTION AT THE MIDSPAN AND (C) SECTION ON THE SHROUD SIDE [14] .....	21
FIGURE 2-4 THE DISTRIBUTION OF A VORTEX STRUCTURE IN GUIDE VANES AND RUNNER. [23] .....	24
FIGURE 3-1: RPT COMPUTATIONAL MODEL AND ITS COMPONENT .....	35
FIGURE 3-2 RUNNER WITH DIFFERENT WRAP ANGLE CONFIGURATION .....	35
FIGURE 3-3 GRID GENERATION FOR RPT MODEL COMPONENTS (A). RUNNER (B). FULL RPT MODEL (C). STAY VANE AND GUIDE VANE .....	37
FIGURE 3-4, COMPARISON OF NUMERICAL AND EXPERIMENTAL DISCHARGE-SPEED (Q11-n11) CURVE.....	38
FIGURE 4-1 MID-SPAN PLANE PRESENTATION.....	40
FIGURE 4-2: VELOCITY STREAMLINES WITHIN RPT TURBO-COMPONENT STAY VANE, GUIDE VANE AND RUNNER INTER-BLADE FLOW CHANNEL WITHOUT INCLUSION OF SPLITTER BLADES AT DIFFERENT OPERATING POINT .....	41
FIGURE 4-3: EVOLUTION OF VELOCITY CURL WITHIN RPT TURBO-COMPONENT STAY VANE, GUIDE VANE AND RUNNER INTER-BLADE FLOW CHANNEL WITHOUT INCLUSION OF SPLITTER BLADES AT DIFFERENT OPERATING POINT .....	42
FIGURE 4-4: PRESSURE CONTOURS WITHIN RPT TURBO-COMPONENT STAY VANE, GUIDE VANE AND RUNNER INTER-BLADE FLOW CHANNEL WITHOUT INCLUSION OF SPLITTER BLADES AT DIFFERENT OPERATING POINT .....	43
FIGURE 4-5: VELOCITY STREAMLINES WITHIN RPT TURBO-COMPONENT STAY VANE, GUIDE VANE AND RUNNER INTER-BLADE FLOW CHANNEL OF OPERATING POINT OF OP 8 AT DIFFERENT WRAP ANGLE OF BLADES.....	44
FIGURE 4-6: EVOLUTION OF VELOCITY CURL WITHIN RPT TURBO-COMPONENT STAY VANE, GUIDE VANE AND RUNNER INTER-BLADE FLOW CHANNEL OF OPERATING POINT OF OP 8 AT DIFFERENT WRAP ANGLE OF BLADES .....	45
FIGURE 4-7: VELOCITY STREAMLINES WITHIN RPT TURBO-COMPONENT STAY VANE, GUIDE VANE AND RUNNER INTER-BLADE FLOW CHANNEL OF OPERATING POINT OF OP 9 AT DIFFERENT WRAP ANGLE .....	46
FIGURE 4-8: EVOLUTION OF VELOCITY CURL WITHIN RPT TURBO-COMPONENT STAY VANE, GUIDE VANE AND RUNNER INTER-BLADE FLOW CHANNEL OF OPERATING POINT OF OP 9 AT DIFFERENT WRAP ANGLE .....	48
FIGURE 4-9 POSITION OF PRESSURE MONITORING POINTS AT DIFFERENT FLOW ZONES (RUNNER, GUIDE VANES AND STAY VANES) .....	49
FIGURE 4-10 POSITION OF PRESSURE MONITORING POINTS ON RUNNER INTER-BLADE FLOW PASSAGE ON SUCTION AND PRESSURE SIDES OF RUNNER BLADE .....	50
FIGURE 4-11: FFT-BASED FREQUENCY SPECTRA OF PRESSURE PULSATION WITHIN THE VANELESS SPACE AROUND THE OUTLET OF SCROLL CASING WITH OPERATING POINT 8 (OP8) AT DIFFERENT WRAP ANGLE WITH SPLITTER BLADES. ....	51
FIGURE 4-12: FFT-BASED FREQUENCY SPECTRA OF PRESSURE PULSATION WITHIN THE VANELESS SPACE AROUND THE INLET OF GUIDE VANES WITH OPERATING POINT 8 (OP8) AT DIFFERENT WRAP ANGLE WITH SPLITTER BLADES (A). NO SPLITTER (B). WA1 (C). WA2 (D). ....	52
FIGURE 4-13: FFT-BASED FREQUENCY SPECTRA OF PRESSURE PULSATION WITHIN THE VANELESS SPACE AROUND THE INLET OF RUNNER WITH OPERATING POINT 8 (OP8) AT DIFFERENT WRAP ANGLE WITH SPLITTER BLADES (A). NO SPLITTER (B). WA1 (C). WA2 (D).....	53
FIGURE 4-14: FFT-BASED FREQUENCY SPECTRA OF PRESSURE PULSATION WITHIN THE RUNNER INTER-BLADE FLOW PASSAGE AT PRESSURE SIDE OF THE RUNNER WITH OPERATING POINT 8 (OP8) AT DIFFERENT WRAP ANGLE WITH SPLITTER BLADES (A). NO SPLITTER (B). WA1 (C). WA2. ....	54
FIGURE 4-15: FFT-BASED FREQUENCY SPECTRA OF PRESSURE PULSATION WITHIN THE RUNNER INTER-BLADE FLOW PASSAGE AT SUCTION SIDE OF THE RUNNER WITH OPERATING POINT 8 (OP8) AT DIFFERENT WRAP ANGLE WITH SPLITTER BLADES (A). NO SPLITTER (B). WA1 (C). WA2 .....	56
FIGURE 4-16: FFT-BASED FREQUENCY SPECTRA OF PRESSURE PULSATION WITHIN THE VANELESS SPACE AROUND THE OUTLET OF SCROLL CASING WITH OPERATING POINT 9 (OP9) AT DIFFERENT WRAP ANGLE WITH SPLITTER BLADES (A). NO SPLITTER (B). WA1 (C). WA2. ....	57
FIGURE 4-17: FFT-BASED FREQUENCY SPECTRA OF PRESSURE PULSATION WITHIN THE VANELESS SPACE AROUND THE INLET OF GUIDE VANES WITH OPERATING POINT 9 (OP9) AT DIFFERENT WRAP ANGLE WITH SPLITTER BLADES (A). NO SPLITTER (B). WA1 (C). WA2. ....	58

FIGURE 4-18: FFT-BASED FREQUENCY SPECTRA OF PRESSURE PULSATION WITHIN THE VANELESS SPACE AROUND THE INLET OF RUNNER WITH OPERATING POINT 1(OP11) AT DIFFERENT WRAP ANGLE WITH SPLITTER BLADES (A). NO SPLITTER (B). WA1 (C). WA2. .... 59

FIGURE 4-19: FFT-BASED FREQUENCY SPECTRA OF PRESSURE PULSATION WITHIN THE RUNNER INTER-BLADE FLOW PASSAGE AT PRESSURE SIDE OF THE RUNNER WITH OPERATING POINT 9 (OP9) AT DIFFERENT WRAP ANGLE WITH SPLITTER BLADES (A). NO SPLITTER (B). WA1(c). WA2. . 60

FIGURE 4-20: FFT-BASED FREQUENCY SPECTRA OF PRESSURE PULSATION WITHIN THE RUNNER INTER-BLADE FLOW PASSAGE AT SUCTION SIDE OF THE RUNNER WITH OPERATING POINT 9 (OP9) AT DIFFERENT WRAP ANGLE WITH SPLITTER BLADES (A). NO SPLITTER (B). WA1 (C). WA2. .... 62

TABLE 1 GEOMETRIC PARAMETERS OF RPT MODEL ..... 34

TABLE 2 GRID DETAILS OF RPT COMPONENTS..... 36

TABLE 3: DETAILS OF SELECTED OPERATING POINTS ..... 39

## Acronyms

RPT	Reversible Pump Turbine
PIV	Particle image Velocimetry
CFD	Computational fluid dynamics
RAS	Reynolds Averaged Navier Stokes Equation
RSI	Rotor Stator Interaction
FFT	First Fourier Transform
RUN	Pressure monitoring point in vane less space zone near runner
SC	Monitoring point around the scroll casing
GV	Monitoring point in guide vane
IBP	Monitoring points on the side of runner
IBS	Monitoring points on the suction side
SST	Shear Stress Transform
BPF	Blade Passing Frequency
VPF	Vane Passing Frequency
GVO	Guide vane opening
OP	Operating point
OC	Operating condition
WA	Name of wrap angle with splitter blades (WA1=120 <sup>0</sup> , WA2=150 <sup>0</sup> )

## NOTATIONS

Q	Flow rate[m <sup>3</sup> /s]
n	Revolution[rev/min]
H	Head[m]
D	Dimeter[m]

## **DEDICATION**

To loving family and friends, who have been unwavering pillars of support and encouragement throughout this journey. Your belief in our abilities has been a constant source of motivation, and we are forever grateful for your love and understanding.

To our esteemed supervisor and mentor whose guidance and expertise have shaped our academic path. Your wisdom and patience have been invaluable, and we are deeply thankful for the knowledge we have gained under your tutelage.

To all the researchers and scholars whose work has laid the foundation for this thesis proposal. Your contributions to the field have been a wellspring of inspiration, and we are honored to build upon your insights

This capstone is dedicated to all those who have touched our lives, directly or indirectly. Your presence has enriched our journey, and it is with profound gratitude and dedication that we embark on this endeavor. May this work contribute positively to our collective understanding and advance the boundaries of knowledge in this field.

# Chapter1 INTRODUCTION

## 1.1 Background

Reversible pump turbines (RPTs) are integral to hydroelectric power generation, capable of operating in three distinct modes: pumping, generating, and phase compensating (idle speed). This versatility makes them vital for achieving power balance and stability in electric power systems, especially in grids dominated by thermal energy. The ability of RPTs to adapt to varying load conditions is crucial in modern energy landscapes, increasingly characterized by the integration of renewable energy sources such as wind, wave, and tidal power.[2]

The evolving technology of RPTs, including the innovative use of splitter blades, aims to improve hydraulic performance and reduce flow instabilities. These advancements are essential for maximizing the efficiency and reliability of RPTs. Researchers have focused extensively on understanding and mitigating flow unsteadiness, examining key instability areas such as flow structure analysis, pressure fluctuations, vortex formation, and impeller-volute interaction. This body of research has produced significant findings that guide the optimization of turbine design and operation.[3]

The complex geometry and dynamic operation of RPTs require careful consideration of system dynamics during the design process. Effective simulation of turbine characteristics is crucial for ensuring flexibility and stability across different modes of operation. Addressing the steep speed-flow characteristics and associated stability issues, particularly at idle speed, is a key aspect of ongoing research and development in this field. [2]

Understanding the complex interactions between the fluid and the turbine components is essential for optimizing the performance of RPTs. Advances in computational fluid dynamics (CFD) and experimental techniques have provided new insights into the behavior of flow within these turbines, allowing for more precise control over their operation. Despite these advancements, challenges remain in fully

understanding and mitigating flow unsteadiness, which can lead to reduced efficiency, increased vibration, and mechanical wear.[3]

This project uses numerical simulations to explore how splitter blades influence the flow and pressure field characteristics within a reversible pump-turbine. The investigation employs a parametric approach, systematically varying the blade wrap angle.

The outcomes of this thesis will contribute to a deeper understanding of the flow dynamics in Reversible pump turbines, enabling engineers and operators to make informed decisions regarding turbine selection, operation, and maintenance. Ultimately, this research has the potential to enhance the efficiency, reliability, and performance of reversible pump turbines across various industrial applications.

## **1.2 Problem statement**

The design and operation of reversible pump turbines (RPTs) are critical to the efficiency and stability of pumped storage power plants, which play a vital role in balancing power supply and demand. One of the most challenging operational zones for RPTs is the S-shape zone, where the turbine operates under part-load conditions and experiences complex flow dynamics that can lead to significant instabilities, efficiency losses, and mechanical stresses.

The blade wrap angle is a design parameter that has been considerably studied in hydraulic pumps, and has been found to exercise a considerable impact on their efficiency. Reversible pump turbines, unlike other conventional turbines, have an absolutely radial runner with long blades completely resembling the pump impeller design, but with larger sizes. However, specific effects of varying the wrap angle on the hydraulic performance and flow stability in reversible pump turbines, especially in the S-shape zone, are not fully understood. This lack of understanding poses a significant challenge to optimizing RPT design for improved efficiency and reliability.

This research seeks to address this gap by conducting a CFD-backed numerical investigation into the impact of runner blade wrap angle on the performance and stability of splitter-bladed RPTs operating within the S-shape zone. The study aims to quantify the effects of different wrap angles on key performance indicators, such as hydraulic efficiency, pressure distribution mode, Runner radial force characteristics and the Rotor-stator interactions. By providing insights into these relationships, the research aims to contribute to the development of more efficient and stable RPT designs, ultimately enhancing the performance of pumped-storage systems.

### **1.3 Main objective**

This research investigates how wrap angle with special blades, called splitter blades, affect water flow and pressure within reversible pump-turbines. These turbines switch between pumping and generating electricity. Traditional blades can struggle with smooth water flow, affecting efficiency. To analyze different blade configurations and operating conditions to understand how wrap angle with splitter blades improve efficiency and stability, ultimately making these turbines even better tools for clean energy production. numerically investigate the impact of runner blade wrap angle on the performance, stability, and flow characteristics of splitter-bladed reversible pump turbines (RPTs) operating within the S-shape zone, with the aim of identifying optimal design parameters for improved efficiency and operational stability

### **1.4 Specific objective of this research include:**

- Analyzing the impact of operating condition on flow and pressure characteristic: Examine how variations in operating conditions, such as speed and flow rate, influence the flow patterns and pressure distribution within the RPT.
- The impact of presence and absence of splitter blade on flow instabilities: Study how the presence or absence of splitter blades affects flow stability within the runner. By comparing flow with and without splitter blades, we can see if they help to make the flow smoother and more efficient.
- Optimizing wrap angle for Flow Stability: Use computer simulations (CFD) to investigate how varying the wrap angle of blades affects the smoothness of water flow within the turbine. This analysis will identify critical points where flow becomes unsteady and how it progresses with different blade configurations. The goal is to find the optimal splitter blade length that minimizes flow instability, ultimately leading to a more stable and reliable turbine operation.
- Create and validate a geometric RPT model using CF Turbo and experimental data.
- Generate and validate the computation grid (grid independence test), using Ansys ICEM and Turbogrid.
- Study how varying splitter blade wrap angles affects flow, pressure, and forces.  
Compare RPT efficiency and power output with and without splitter blades

## **1.5 Research questions:**

- Do varying splitter blade wrap Angle influence how flow instabilities develop and worsen within the RPT?
- Compared to no splitter blades, how effectively do splitter blades improve the smoothness of water flow within the turbine?
- How do operating conditions (flow rate, speed) affect flow instability development and intensity
- What factors affect the grid independence for the computation grid generated in Ansys ICEM and TurboGrid?
- How do splitter blades affect RPT performance in the S-shape zone?
- How do varying splitter blade wrap angles affect flow, pressure, and force characteristics?
- How do splitter blade wrap angles influence RPT efficiency and power output?

## **1.6 Justification**

Academically, the findings will expand our understanding of fluid dynamics within these complex machines, informing future research and development in pump turbine design. Practically, the project will provide valuable insights for manufacturers and operators leading to increased turbine efficiency for energy savings and cost reductions, and ultimately, a more sustainable approach to fluid transportation through efficient pumping systems.

## **1.7 Scope**

This research investigates flow instability in reversible pump turbines, focusing on the impact of splitter blades and their varying wrap angles on flow behavior and using computational fluid dynamics (CFD) to investigate how varying runner blade wrap angles impact the performance and stability of splitter-bladed reversible pump turbines (RPTs) operating within the S-shape zone. Will not delve into areas already explored by other studies, such as cavitation formation, fluid-structure interaction, rotating stall, and associated energy losses within these turbines.

## **1.8 Report outline**

This report has five chapters. The introduction, literature review, the methodology, conclusions, and the recommendations. Introduction provides a comprehensive overview of reversible pump turbines (RPTs). It will begin by explaining the fundamental principles behind RPTs, outlining their key components and functionalities. The chapter will then delve into the importance of studying flow instabilities within RPTs

The literature review section of this research explores the basic concepts of Reversible pump turbine, work conducted by various researchers on flow instabilities in pump turbines with or without splitter blades. The literature review will also identify any gaps in the existing knowledge, creating a foundation for our current research and highlighting the significance of our study in addressing these gaps.

The Methodology chapter begins by providing an overview of commonly used methods employed by other researchers in related fields. The chapter will describe the chosen numerical simulation process in detail. This description will encompass the design of the model used in the simulations, the process of mesh generation, and the overall procedures involved in simulating the flow within the RPT.

Chapter 4 will present and analyze the results obtained from the numerical simulations conducted in the previous chapter exploring their implications for understanding flow behavior and performance within the RPT. This analysis will be crucial in drawing meaningful conclusions about the impact of the chosen methodology and the effectiveness of splitter blades in mitigating flow instabilities.

Chapter 5 will summarize the key findings of your research. This will involve highlighting the achieved goals outlined in the introduction and the final chapter will offer recommendations for future research based on our findings and the identified knowledge gaps highlighted in the literature review.

## Chapter2 LITERATURE REVIEW

### 2.1 Basic concept

A reversible pump turbine, also simply called a pump turbine, is a versatile engineering machine that can act as both a pump and a turbine, offering incredible flexibility in hydropower applications [4]:

- **Pump Mode:** In this mode, the turbine operates like a pump. It uses an external power source, typically electricity, to spin the blades. This rotation forces water from a lower reservoir to a higher one, like a conventional water pump. This is useful for applications like transferring water for hydroelectric power plants or irrigation systems.
- **Turbine Mode:** When the flow of water is reversed, the pump turbine acts as a turbine. The flowing water pushes against the blades, causing them to spin and generate electricity. This mode is often used in hydroelectric power plants where flowing water drives the turbine to produce electricity.

The key advantage of a pump turbine is its reversibility. It can switch between pumping and generating electricity depending on the needs of the system. This makes them ideal for applications where both functions are required, such as pumped storage hydroelectric plants

#### 2.1.1 History of A Reversible Pump Turbine

Harnessing the power of water has been a cornerstone of human civilization for millennia. In the 20th century, this relationship took a significant leap forward with the development of hydroelectric power generation and, in turn, reversible pump turbines (RPTs). This chapter is about the rich history of RPTs, exploring their evolution from early concepts to the advanced machines that play a vital role in modern energy management.[5]

The story of RPTs begins with the fundamental idea of using water to store and generate electricity. This concept emerged in the early 20th century, fueled by the growing demand for reliable and efficient energy

sources. The first large-scale applications of pumped-storage hydroelectricity appeared in the 1930s. These pioneering projects aimed to provide a means of storing excess electricity during off-peak hours and generating power during peak demand periods, thereby achieving a crucial balance for electrical grids. While pumped storage offered an innovative solution, it required a key technological component – the reversible pump turbine. The mid-20th century witnessed the birth of this revolutionary machine. One of the earliest successful implementations was at the Ffestiniog Power Station in Wales, which became operational in 1963. The Ffestiniog project demonstrated the feasibility of using a single machine for both pumping and generating functions. This breakthrough significantly enhanced the efficiency and flexibility of hydroelectric power plants.[5]

The latter half of the 20th century saw a surge in the adoption of RPTs. This growth was driven by the increasing demand for energy storage solutions that could complement the growing share of intermittent renewable energy sources, such as wind and solar power. By the 1980s and 1990s, RPTs were being integrated into numerous pumped-storage facilities around the world. These facilities became vital tools for grid stability and energy management, ensuring a reliable electricity supply despite the fluctuations inherent in renewable energy sources.[6]

The design and performance of these machines have constantly evolved, fueled by advancements in materials science, fluid dynamics, and computational modeling. Early designs prioritized robust construction and basic hydraulic performance. However, as the understanding of fluid dynamics deepened, more sophisticated designs emerged. One of the most significant advancements in RPT technology was the introduction of splitter blades. These smaller blades, positioned strategically between the main impeller blades, were designed to improve flow uniformity and reduce hydraulic losses. This innovation has been instrumental in enhancing the performance of RPTs by mitigating issues like flow separation and secondary flow phenomena, which can lead to inefficiencies and increased mechanical stress. The introduction of splitter blades in commercially available RPTs began in earnest in the late 20th century and has continued to evolve into the 21st century. Leading companies specializing in hydroelectric equipment, such as Voith Hydro and Andritz Hydro, have been at the forefront of incorporating splitter blade technology into their RPT designs. These advancements have undergone rigorous testing and validation to ensure they meet the stringent performance and reliability standards required for hydroelectric applications.[7]

The importance of RPTs extends beyond their ability to store and generate electricity efficiently. These machines also play a crucial role in regulating functions, essential for achieving power balance in electric power systems. This is particularly critical in grids dominated by thermal energy sources, where RPTs enhance overall governor stability. The rise of new renewable energy sources, such as wind, wave, and tidal power plants, necessitates better regulation capabilities of traditional power suppliers. RPTs play a vital role in addressing this challenge.[8]

### 2.1.2 Reversible pump Turbine components

RPTs function effectively, let's explore their key components: The **runner**, a propeller-like structure, acts as the heart by accelerating water flow. Adjustable **guide vanes** upstream regulate incoming flow, while the **spiral casing** collects and converts the high-velocity water into pressure. In turbine mode, a **draft tube** further recovers energy downstream. A robust **shaft** with high-quality **bearings** supports the runner, and **seals** prevent leakage. Finally, the **drive mechanism**, an electric motor in pumping mode and water flow in turbine mode, completes the picture, enabling RPTs to excel in both pumping and generating duties.[5]

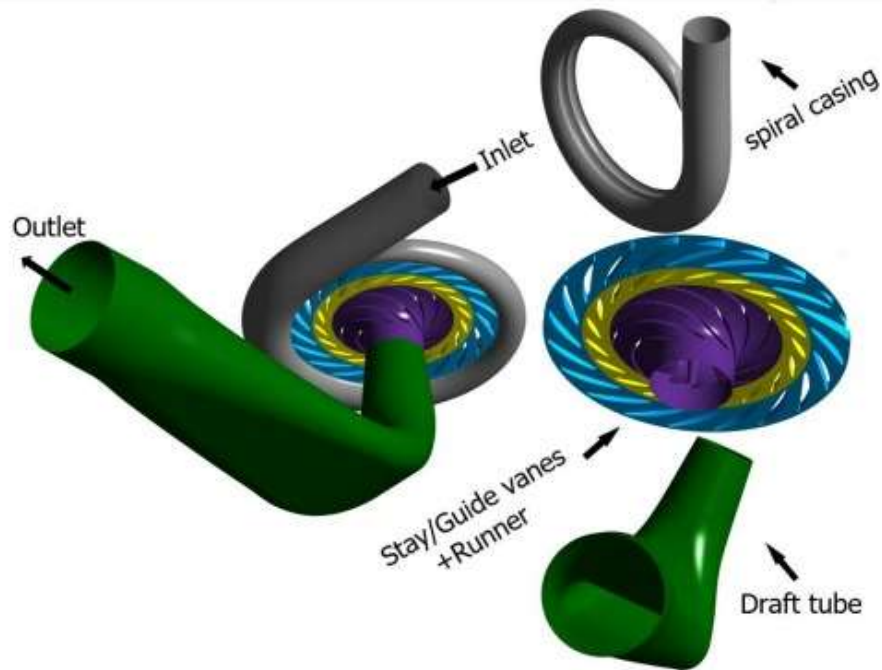


Figure 2-1 Figure 1 Reversible Pump Turbine components[9]

### 2.1.3 Classifications of Reversible pump Turbine

There are two main types of reversible pump turbines, each with its own strengths:[5]

- Francis Pump Turbine:** This is the most common type. It features a spiral casing and a mixed-flow impeller with diagonally oriented blades. It offers high efficiency across a wide range of operating conditions, making it suitable for various applications.
- Kaplan Pump Turbine:** This type utilizes an adjustable-pitch propeller design for its impeller. By adjusting the blade angles, the efficiency can be optimized for different flow rates and head pressures in both pump and turbine modes. Kaplan turbines are particularly well-suited for situations with fluctuating water flow or head conditions.

### 2.1.4 Reversible Pumps application

Reversible pump turbines (RPTs) are the workhorses behind pumped storage hydropower, offering a multi-faceted solution. Their key applications include:

- **Pumped Storage Hydropower:** RPTs store excess energy during off-peak hours by pumping water uphill, then generate electricity during peak demand. This stabilizes the grid and reduces reliance on expensive peak power plants.
- **Irrigation Systems:** RPTs reliably pump water to higher elevations for irrigation, especially valuable in arid regions.
- **Flood Control:** They quickly pump floodwater away, mitigating risk and protecting infrastructure.
- **Desalination Plants:** RPTs provide a reliable source of seawater for desalination, increasing water security in areas with limited freshwater resources.

Beyond these core applications, RPTs are seen as key players in integrating renewable energy and creating a more sustainable energy future.[5]

### 2.1.5 Pump operating conditions.

Reversible pump turbines (RPTs) operate under two distinct modes: pumping and turbine. Each mode has its own set of operating conditions and performance characteristics that are crucial for efficient operation.

#### **Pumping Mode:**

- **Head:** This is the difference in elevation between the water source (lower reservoir) and the destination (upper reservoir) that the RPT needs to overcome.
- **Flow Rate:** This is the amount of water pumped per unit time, typically measured in cubic meters per second ( $m^3/s$ ).
- **Rotational Speed:** The speed at which the runner rotates, usually expressed in revolutions per minute (RPM). This can be adjusted to optimize pump efficiency.
- **Power Input:** The amount of electrical power required to drive the pump.

## **Turbine Mode:**

- **Head:** This is the difference in elevation between the water source (upper reservoir) and the tailrace (downstream water body) that drives the turbine.
- **Flow Rate:** This is the amount of water flowing through the turbine per unit time ( $\text{m}^3/\text{s}$ ).
- **Rotational Speed:** The speed at which the runner rotates due to the water flow, impacting electricity generation. This speed can be adjusted to match grid requirements.
- **Power Output:** The amount of electrical power generated by the turbine.

## **2.2 Similar works**

### **2.2.1 Pump-Turbine Performance Improvement**

Li et al.[10] investigated the impact of splitter blades on pump-turbine performance in pump mode. This study employed numerical calculations to analyze the performance and internal flow characteristics of pump-turbines with and without splitter blades. The results indicate that splitter blades contribute to a higher head in pump mode due to factors like larger tangential velocity at the runner outlet and increased pressure at the trailing edge of the pressure side. Additionally, the use of splitter blades led to reduced backflow at the runner outlet, lower entropy generation rates, and a more favorable vorticity distribution compared to the design without splitter blades.

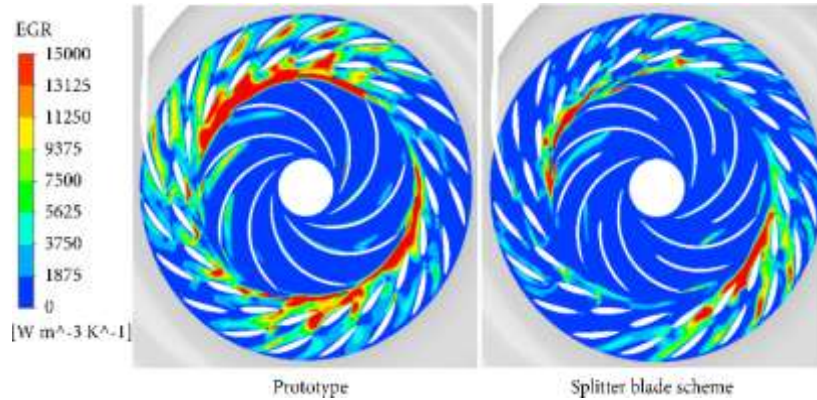


Figure 2-2 The contours of entropy generation rate distribution at mid span for both schemes.[10]

Olimstad et al. [11] shifted the focus to runner geometry, a paramount factor influencing turbine mode efficiency. They studied the relationship between runner geometry and the performance of reversible pump turbines (RPTs) in turbine mode. Their research involved measurements on a physical model with five different leading-edge profiles for the runner blades. These profiles varied the inlet blade angle and the radius of curvature. The study found that the RPT exhibited steeper flow-speed characteristics in turbine mode compared to a typical Francis turbine. This difference was attributed primarily to the geometry of the inlet blade section, where the RPT blades have a much smaller angle compared to Francis turbines. The researchers tested two different blade angles and conducted simulations on four variations. Both the physical and computational analyses revealed that a smaller blade angle resulted in less steep characteristics in turbine mode. However, this also led to a more pronounced "s-shape" in the performance curve, which can be problematic. Interestingly, they also observed that leading edges with a longer radius of curvature exhibited fewer steep characteristics.

As energy loss remains a persistent challenge in pump-turbines, Gui et al. [12] investigated how high-head pump-turbines with splitter blades lose energy, aiming to improve overall efficiency. Traditional methods for calculating these losses were found to be limited. By employing simulations and experiments, the study revealed that higher water pressure leads to slower efficiency decline. Interestingly, the biggest energy losses occur in areas with sharp velocity changes behind the splitter blades, not from whirlpools within the runner. Furthermore, flow conditions within the runner were shown to impact losses in the draft tube. In conclusion, optimizing splitter blade design and managing runner flow patterns are critical for minimizing energy losses in these high-head pump-turbines.

Yuan et al. [13] added another compelling chapter by using splitter blades to improve high-speed centrifugal pumps. Pumps with splitter blades showed significant improvement in efficiency (nearly 4%) and head (10 meters) compared to a standard pump. These improvements stemmed from better flow characteristics achieved by the splitter blades: reduced flow separation, enhanced jetting flow, and improved stability through lower turbulence. The splitter blades also significantly reduced pressure fluctuations within the pump, leading to steadier flow. However, increasing the splitter blade length beyond a certain point yielded no additional benefits, and the design should favor a bias towards the main blade's suction surface for optimal flow area. Overall, this study highlights splitter blades as a promising technique to boost performance and stability in high-speed centrifugal pumps, while also providing valuable design considerations.

### 2.2.2 Flow Behavior and Instability in Pump-Turbines

Linsheng et al [14] act as our initial guides, employing computational simulations to illuminate the flow behavior within the S-shaped zone. Their investigation unveils the presence of unique backflow vortex structures forming around the runner inlet, exhibiting a dynamic shift depending on the operating point. This backflow intensifies the interaction between rotating and stationary components, as shown in (Fig 3) consequently leading to pressure fluctuations. Interestingly, the study suggests that a distinct phenomenon, rotating stall, is the culprit behind uneven pressure fluctuations observed at lower frequencies

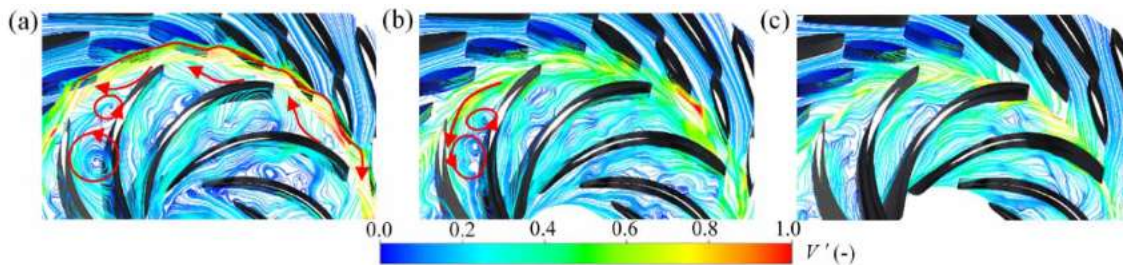


Figure 2-3: Streamlines on the three spanwise sections when the BFVSs occur on the hub side ( $15^\circ$  GVO). (a) Section on the hub side, (b) section at the midspan and (c) section on the shroud side [14]

Binama et al [15] used simulations to investigate the emergence of flow instabilities and pressure pulsations arising in reversible pump turbines (RPTs) under off-design conditions. Low torque operation

and backflow in the vaneless space were identified as the cause behind these instabilities, which contribute to the S-shape seen in RPT performance curves. Interestingly, increasing guide vane opening reduced runner flow instability but worsened pressure pulsations across the RPT, with the vaneless space being most susceptible to GVO changes.

Adopting a different approach Lenarcic et al. [16] highlighted the fundamental pumping characteristic of the runner as the cause behind S-shape instabilities in reversible pump-turbines. using a combined approach of theory, simulations, and experiments. Their goal was to understand the root causes of these instabilities and develop strategies to improve operational stability. This suggests focusing on the instability symptoms - vortices within the turbine - rather than modifying the runner itself. The study identified vortex behavior under different operating conditions and explored mitigation strategies like misaligned guide vanes, variable runner speed (with limitations), lowered runner outlet pressure, and optimized rotor-stator distance. These findings can guide the development of more stable and efficient reversible pump-turbines without requiring major design changes.

The narrative takes an surprising turn as Dong et al.[17] investigated the performance of a splitter blade pump-turbine in pump mode, focusing on the efficiency dip and anomalous curve behavior observed at certain flow rates. Entropy production analysis revealed that energy losses were mainly concentrated in the runner, particularly at the trailing edge of long blades in the vaneless space, differing from traditional pump-turbines. Interestingly, splitter blades were found to reduce vortex formation and improve overall energy performance compared to traditional designs. These findings confirm the existence of hump and hysteresis effects in splitter blade pump-turbines, identify loss mechanisms, and provide valuable insights for optimizing design and ensuring stable operation.

Yasa et al.[18] introduced a new multi-splitter vane design for turbine stators. While the design matched conventional efficiency at ideal conditions, it was highly sensitive to incoming flow angle variations. Splitter vanes suffered significant performance drops due to flow separation when the flow deviated from the design angle. The study also introduced a novel method to analyze losses in these vane configurations by examining individual flow passages. This research suggests promise for the multi-splitter vane design at specific operating conditions but highlights the need for addressing sensitivity issues before widespread adoption.

Lai et al. [19] investigated flow patterns inside a high-head pump-turbine draft tube using LDV (Laser Doppler Velocimetry) measurements and visualization. They compared the measurements to hydraulic design and model tests, finding good agreement. LDV effectively captured flow features like axial/tangential velocities, backflow zones, and vortex rope behavior. The technique is useful for analyzing swirl intensity, backflow, and vortex rope location, aiding in pump-turbine design and operation. Future studies combining LDV with PIV (Particle Image Velocimetry) could provide more detailed information on the 3D flow field and vortex structures.

### **2.2.3 Pump-Turbine Stability and Pressure Pulsations**

Xiao et al.[20] investigated pressure pulsations, a major contributor to vibration in pump turbines, under runaway conditions using the Hilbert Huang transform, a powerful signal processing technique. This method provided a more comprehensive analysis compared to traditional FFT methods. Their simulations revealed that the main pressure pulsation frequencies in the vaneless region shifted from a complex mix to a blade passing frequency dominant distribution during runaway. The draft tube exhibited vortex rope frequency as the strongest contributor, along with rotational and blade passing frequencies. Furthermore, the study suggests propagation of these characteristic frequencies upstream and downstream within the turbine, highlighting the importance of understanding pressure variations for safe and reliable pump turbine operation

Li et al.[21] studied modifying runner blades in pump-turbines to dampen pressure fluctuations during hump operation, which can lead to vibration and instability. They investigated increasing the runner outlet angle or radius near the shroud. Both modifications reduced pressure fluctuations, with an increase in radius being most effective. The culprit behind these fluctuations was identified as rotating low-pressure regions near the guide vanes. The design changes reduced stall vortices in these areas, enhancing flow stability. Additionally, they lowered the amplitude of the dominant low-frequency pressure fluctuations. Notably, increasing the runner radius resulted in the most uniform pressure distribution.

Mao et al. [22] investigated a self-adaptive closure law for guide vanes in pump-turbines to improve stability during load rejection in pumped storage plants (PSPs). Load rejection can cause dangerous fluctuations in speed and pressure. Their optimized closure law, based on a current PSP design and incorporating speed and pressure variations, reduced these fluctuations in simulations. The study also revealed that rotor-rotor interaction strengthens pressure fluctuations near the runner. Future work will consider real-world variations in PSPs and explore non-linear closure laws.

Investigating the influence of water flow on the structure of a pump-turbine under no-load conditions. Ren et al. [23] used computer simulations to analyze how water swirls and pressure pulses affect the turbine's parts. The study found that under no-load, the water flow becomes unstable and forms swirls inside the runner blades. As the guide vane opening (GVO) increases, these swirls move and cause pressure pulses throughout the turbine. These pressure pulses stress the runner blades unevenly, concentrating stress at the base where cracks are likely to form. This explains cracks observed in real-world turbines. The study suggests that to avoid such damage, pump-turbines should ideally not operate under no-load conditions with large GVO. In future designs, the runner and guide vanes should be considered together to improve how they handle water flow and minimize stress.

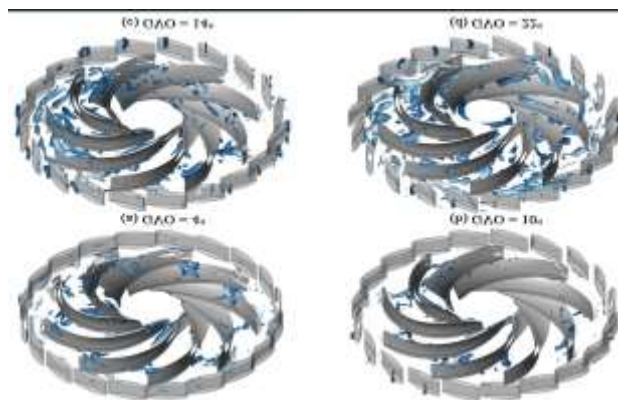


Figure 2-4 The distribution of a vortex structure in guide vanes and runner.[23]

## 2.2.4 Pump-Turbine Operation and Design

This study by Wang et al.[24] simulated the closure of wicket gates in a pump-turbine operating in pump mode. They used a 3D transient simulation to analyze the effects of gate closure on performance. The closure creates a time lag between gate position and changes in flow rate and power. Downstream of the

wicket gates, pressure fluctuations are significant, especially during mid-closure. The study suggests that wicket gate closure strategies should consider minimizing torque on the wicket gates

## **2.3 Summary of previous works and their Gaps**

Pump-turbines, the workhorses of renewable energy storage, demand meticulous design and operation to achieve optimal performance and stability. This part explores how operating conditions and design choices significantly impact pressure pulsations, rotating stall, efficiency, and the occurrence of the hump characteristic. It also identifies key knowledge gaps that future research can address.

### **2.3.1 Influence of Operating Conditions and Design:**

Hu et al. [25] investigated pressure pulsations within a pump-turbine design featuring splitter blades. Their research focused on how these pulsations change with varying water flow rates. At high flow rates, the dominant pressure pulse frequency corresponds to half the total number of runner blades. However, as the flow rate decreases, a different frequency – linked to the total number of blades – becomes dominant. This shift in dominant frequency is a key finding, as it differs from what's observed in conventional pump-turbines. The authors emphasize the importance of considering this phenomenon in pumped storage power stations to avoid potential structural issues caused by fluctuating pressure. For further understanding of pressure pulsations and blade design optimization, future research could explore additional factors beyond flow rate, such as the specific geometry of the splitter blades themselves.

Investigating the transient effects of closing wicket gates in a pump-turbine operating in pump mode. Wang et al.[26] used a novel dynamic mesh technique to simulate the closure process and analyze the resulting flow characteristics. Closure creates a time lag between gate position and changes in flow rate and power. Downstream of the wicket gates, pressure fluctuations are significant, especially during mid-closure. The study suggests that wicket gate closure strategies should consider minimizing stress on the wicket gates and runner blades. Future work could explore different closure patterns to improve efficiency and stability.

The review by Zhang et al.[27] examined rotating stall, a source of instability, in reversible pump turbines operating in generating mode. It occurs at off-design conditions and can lead to failed starts, pressure fluctuations, and vibrations. The stall initiates at runaway and worsens at low discharge conditions. Its signature effects include pressure fluctuations, flow blockage, and backflow, all contributing to instability. The article discusses methods for identifying rotating stall but acknowledges a gap in knowledge regarding optimal identification methods in real-world applications. Future research is encouraged to explore preventative measures to avoid rotating stall or mitigation strategies to minimize its impact on turbine performance.

Meng et al. [28] Investigated the influence of splitter blades on pressure pulsations within high-head turbines [1]. Splitter blades are commonly used to improve efficiency and stability. Here, the researchers use computer simulations to analyze pressure fluctuations at different operating conditions within a high-head turbine runner with and without splitter blades. They compared runner designs with different splitter blade lengths to efficiency, pressure distribution on the blades, and the amplitude of pressure pulsations. The results showed that splitter blades can significantly improve efficiency, with the optimal length being 75% of the main blade length. However, splitter blades also affect pressure pulsations by altering the flow and introducing additional blade interactions. The study identified a design with a splitter blade length of 82.5% of the main blade as a good compromise, improving pressure characteristics without significantly sacrificing efficiency. However, the study relies solely on simulations, and future research incorporating real-world testing could strengthen the findings. Additionally, the long-term effects of these design modifications on factors such as blade erosion or vibration require further investigation.

Li et al. [29]examines the hump characteristic, a source of instability in pump-turbine operation during pumping mode. The hump characteristic refers to a region of inefficiency and instability that can occur at certain operating conditions. The researchers use a combination of experimental testing and computer simulations to analyze the flow dynamics within the turbine during hump operation. They identify three vortex groups that form within the turbine under these conditions and vary in strength and location depending on the flow rate. The study suggests that understanding these vortex groups is crucial for improving pump-turbine stability. However, the study does not explore methods to mitigate the effects

of these vortex groups. Additionally, future research could benefit from incorporating economic considerations to assess the feasibility of implementing any proposed solutions.

### **2.3.2 Pressure Fluctuations and Turbine Stability**

Fu et al. [30] investigated the source of complex, low-frequency pressure fluctuations that occur during a pump-turbine's load rejection process. While the process itself is known to be complex, the origins of these pressure fluctuations have remained unclear. Here, the authors use a validated 3D simulation to analyze the transient flow and identify three key factors contributing to the pressure fluctuations: water hammer within the turbine, localized reverse flow near the runner inlet, and the formation of a three-dimensional blocking water ring in the vaneless space. Understanding these factors and their interactions can aid in future efforts to mitigate or eliminate these pressure fluctuations during load rejection. However, the study relies solely on simulations, and future research incorporating real-world testing could strengthen the findings.

Simulating Flow Characteristics Across Operating Modes, Hu et al. [31] studied the flow characteristics and pressure pulsations within a pump-turbine across five different operating modes. Their goal is to understand how these factors change depending on the turbine's operation. Using computer simulations, the researchers analyzed the water flow, pressure, cavitation, and forces acting on the turbine's blades. They found that smoother operation and less cavitation occur when the turbine operates near its design points for pumping or generating electricity. In contrast, significant pressure fluctuations and cavitation arise when the turbine works outside these ideal zones. The pump-brake mode, where the turbine operates like a pump but wastes energy, creates the most concerning conditions. Here, violent water flow creates substantial pressure variations and forces on the turbine blades, potentially leading to harmful vibrations. The study recommends avoiding long-term operation in these unfavorable modes and using the findings to guide future research on pressure fluctuations and turbine blade design. The current study utilizes computer simulations, providing valuable insights but limiting the ability to account for real-world complexities. Including experimental validation in future research would strengthen the findings and improve generalizability to actual pump-turbine operation. Additionally, while the study identifies unfavorable operating modes, a cost-benefit analysis could be helpful in determining the economic implications of prioritizing operation within the ideal zones.

Fu et al. [32] examined the dynamic behavior of pump-turbines experiencing runaway conditions with large variations in water pressure. Runaway refers to a situation where the turbine loses control and keeps spinning at an increasing speed. Simulating and analyzing such scenarios is challenging due to difficulties in setting accurate starting conditions and identifying the origin of pressure fluctuations. The researchers address this by proposing a combined one-dimensional and three-dimensional simulation approach that considers water dynamics. Their analysis reveals two distinct fluctuation components in pressure and forces acting on the turbine blades. One component occurs at a frequency roughly three times the turbine's rated rotation speed. The other is a series of whole-number multiples of the rotational frequency, unrelated to rotor-stator interaction. Understanding these components is crucial for controlling pressure fluctuations during runaway events. However, the study relies solely on simulations, and future research incorporating real-world testing could strengthen the findings.

## **2.4 Chapter conclusion**

This literature review presents a comprehensive overview of reversible pump turbines, covering their history, types, characteristics, and essential parameters, highlighting their significant applications across various industries. It explores the evolution of pump turbine technology, tracing its development from ancient civilizations to the modern era, showcasing its remarkable progress. Moreover, the review explores flow instabilities in reversible pump turbines, summarizing prior research and identifying gaps and limitations in the existing knowledge. Its findings provide a solid foundation for future research and innovation in the field, fostering further improvements and breakthroughs RPTs design and operation.

## **Chapter3 METHODOLOGY**

### **3.1 Previous methods**

The methods used in investigation of flow instabilities in fluid mechanics or dynamics are classified into experimental and numerical methods. Experimental methods involve physical testing of pumps, which can be expensive and time-consuming, and numerical methods utilize computational simulations to analyze flow behavior within pumps.

Historically, research into flow instabilities within hydroelectric machines relied on experimental methods due to limitations in computational power and numerical code accuracy. These experimental methods provide valuable real-world data on how flow behaves under different operating conditions, allowing visualization of complex flow patterns and disruptions that numerical methods might struggle to capture, and the flexibility to test pumps under a wider range of conditions, including unexpected scenarios or extreme situations.

#### **3.1.1 Experimental methods**

Focusing on the flow instabilities in a reduced scale model of a pump-turbine during generating mode at off-design conditions Hasmatuchi et al.[33]. focused on the phenomena of runaway and S-shape scenarios. The research utilizes wall pressure measurements within the stator using 30 miniature piezoresistive sensors. The experimental method involves increasing the runner speed from the best efficiency point and analyzing the pressure fluctuations and spectral content.

Lai et al. [19]employed Laser Doppler Velocimetry (LDV) and vortex rope visualization to investigate the intricate flow patterns within the draft tube of a high-head pump-turbine. Their focus centers on various operating conditions, including off-design scenarios, for both turbine and pump modes. Measurements were conducted across a range of speeds and loads to analyze factors like swirl intensity, backflow regions, and vortex rope behavior. The LDV technique proved instrumental in precisely characterizing these flow features and their connection to the pump-

turbine design. This research offers valuable data for understanding and optimizing pump-turbine performance across diverse operating regimes

Qin et al. [34] investigated the improvement of hydraulic performance in a pump-turbine through an experimental approach. The research focuses on eliminating the unsteady "hump" and "S" characteristics that occur during turbine and pump operation, respectively. These characteristics are believed to be linked to complex vortex patterns in the vaneless region. The researchers designed and tested a scaled runner with an optimized high-pressure side (HPS) using a multi-objective optimization process. This design aimed to eliminate the unsteady characteristics while maintaining efficiency. Hydraulic experiments compared the optimized runner to the original design. The results showed a slight trade-off in efficiency (0.1% decrease in turbine mode, 0.1% increase in pump mode) but significant improvements in other aspects. The S margin (operating range free from the "S" characteristic) increased, and pressure fluctuations in the vaneless region were reduced by up to 33.3% (turbine mode) and 21.4% (pump mode)

Using Particle Image Velocimetry (PIV) to investigate the flow field within a high-head pump-turbine model, Liu et al. [35] focused on key operational challenges faced by pump-turbines, including the S-shape and hump problems, pressure fluctuations, and cavitation. PIV experiments were conducted under various typical operating conditions to analyze the internal flow patterns and vortex behavior. The results suggest a strong correlation between these operational issues and the distribution of vortices within the flow field.

Deng et al. [36] investigated the flow characteristics within the draft tube of a model Francis pump turbine using Laser Doppler Velocimetry (LDV). The research focuses on pressure pulsations within the draft tube, which are believed to be linked to the formation of a cavitating vortex rope. The researchers measured the velocity distribution across the draft tube under various cavitation coefficient conditions. Their findings indicate a direct relationship between pressure pulsations and velocity pulsations within the draft tube. Additionally, they observed that the main frequency of these velocity pulsations increased with a higher cavitation coefficient.

Han et al. [37] explored the characteristics and development of tip leakage cavitation, a major concern in hydraulic machinery. Using high-speed visualization on closed loop test rig, they identified two primary categories of tip leakage vortex cavitation and observed a novel double hump structure under severe cavitation conditions. The research details the four stages of the double-hump cavitation's evolution and its relationship with NPSH. The findings include empirical

functions describing the impact of NPSH on projected area, axial thickness, and circumferential length of the cavitation.

Zhang et al. [38] investigated the causes of performance discontinuity, a phenomenon that disrupts stable operation in pump-turbines during pumping mode. Their findings suggest that pre rotation is the primary factor for this instability, and the impeller design plays a crucial role. The researchers employed experiments with varying diffuser vane openings results indicate that flow recirculation at the impeller inlet coincides with the point of discontinuity in the performance curve.

Ji et al. [39] explored how the flow characteristics within the draft tube of a Francis turbine change under different operating conditions. The research focuses on a Francis turbine and uses an experimental measurement using Laser Doppler Velocimetry (LDV). Three guide vane openings (20%, 100%, and 120%) were investigated at both rated and maximum head conditions. The results indicate that a large, diffuse vortex present at the draft tube inlet transforms into a more well-defined vortex rope as the guide vane opening increases. This change is accompanied by significant improvements in pressure, velocity, and overall flow characteristics within the draft tube.

Vagnoni et al.[40] investigated the impact of a rotating air-water mixture on the pressure and torque stability of a reversible pump-turbine in condenser mode.. The researchers established specific operating conditions: closed guide vanes, compressed air injected into the draft tube to reduce impeller friction, and cooling water discharge through labyrinth seals. They employed high-speed visualizations alongside pressure and torque measurements. This combined approach allows them to connect the air-water ring's behavior within the gap between the impeller and guide vanes to pressure and torque fluctuations. The study utilizes techniques like cross-spectral analysis and phase averaging to analyze the periodicity of these instabilities

### **3.1.2 Numerical methods**

Scientists have studied how fluid flows inside pump turbines by running experiments and using numerical methods as shown in the above reviews. While experiments are helpful, they can be

slow and time-consuming and improving the machine performance at design and off design conditions would be difficult if we rely on experimental methods alone. Luckily, computers advanced, and scientists are developing better programs to analyze fluid flow. This means they can increasingly rely on computers to understand how fluid moves in turbines and make them work better, and efficiently.[41]

Li et al. [21] explores two design strategies for the high-pressure edge of pump-turbine runner blades to reduce pressure fluctuations within the hump region. This region is known for causing instability and vibrations in pump-turbines. They employed Large Eddy Simulation (LES) validated with experimental data to analyze the effectiveness of these strategies. The research suggests that both approaches reduce stall vortices and the "rotating stall phenomenon, which are the primary culprits behind the pressure fluctuations.

LI et al. [42] investigated the unsteady flow characteristics within a centrifugal pump equipped with splitter blades using numerical simulations validated with experimental data. Their focus was on a low-specific-speed pump, and they employed ANSYS-CFX software coupled with the Shear Stress Transport (SST)  $k-\omega$  turbulence model. The simulations analyzed pressure fluctuations throughout the pump, revealing variations in frequency depending on the location relative to the volute tongue.

Ješe et al. [43] employed CFD simulations to investigate the hump instability, a performance issue in pump-turbine pump mode. This instability results in a hump-shaped efficiency curve and can cause vibrations and losses. Their study uses a high-head pump-turbine model to analyze the effects of guide vane opening angles and flow rates on the hump and associated rotating stall (internal flow separation). Simulations were conducted with various boundary conditions including constant mass flow rate at the inlet and static pressure at the outlet. The  $k-\varepsilon$  turbulence model with extended wall functions was used within the FINETM/Turbo software for the simulations.

Guo et al. [44] investigated cavitation in a high-speed centrifugal pump equipped with a splitter-blade inducer using a combined approach of numerical simulations (ANSYS-CFX) and

experimental testing. Their focus was on analyzing the vapor volume fraction and cavitation development within the pump. They observed significant cavitation within the impeller without the inducer, whereas the splitter-blade inducer substantially reduced cavitation, primarily concentrated on the suction side of a single impeller passage. The simulations employed a two-phase mixture model with the RANS equations and revealed three stages of cavitation development in the impeller: slow development, rapid growth, and backward extension.

Yan et al.[45] employed computational fluid dynamics (CFD) to investigate the off-design hydrodynamics of a low specific speed, Francis-type pump-turbine model. Their focus was on turbine mode operation, specifically analyzing runaway conditions, the "S-shaped" turbine brake curve at low discharge, and low positive discharge scenarios. using ANSYS-CFX 13 software for the simulations, leveraging the standard  $k-\epsilon$  turbulence model. A completely structured hexahedral mesh was generated with ANSYS-ICEM software. The study successfully captured the flow instabilities that occur during transitions to run away and turbine brake modes, including rotating stall phenomena observed at low discharge conditions.

Dong et al. [17] focused on a splitter blade pump-turbine operating in pump mode. Their research investigated the hump characteristic and hysteresis effect, which are performance instabilities observed in the pump's efficiency curve. The simulations analyze pump behavior with small guide vane openings. ANSYS Fluent 2021 R1 software is used for CFD simulations employing the SST  $k-\omega$  turbulence model. To capture the unsteady flow characteristics, the simulations utilize velocity inlet and pressure outlet boundary conditions with turbulence intensity set at 5% at the inlet.

Braun et al.[46] employed CFD simulations (CFX-5.7) to investigate an efficiency drop observed in a specific pump-turbine ( $n_q=66$ ) operating as a pump. This inefficiency appears as a saddle point in the pump's energy-discharge curve. The study utilizes a reduced model with one channel per component and analyzes part-load operation with various flow rates. Simulations were conducted with constant pressure at the inlet and specified mass flow rate at the outlet. The Menter-SST turbulence model is chosen for its ability to handle both free shear flow and near-wall regions. The mesh generation utilizes a block-structured, hexahedral approach with particular attention paid to smooth transitions and appropriate  $y^+$  values for wall treatment.

Zhu et al.[47] presented a Mult objective optimization method to design a high-efficiency and stable runner for a reversible pump-turbine. This type of machine needs to excel in both pump and turbine modes due to frequent operational switching. Their approach utilizes 3D inverse design to generate blade geometry based on specified performance goals. Computational fluid dynamics (CFD) simulations evaluate different designs, but the number of simulations is reduced using Design of Experiments (DoE). Response Surface Methodology (RSM) establishes relationships between design parameters (blade loading, blade lean angle, and channel shape) and performance objectives (efficiency and stability). Finally, a Mult objective Genetic Algorithm (MOGA) finds optimal solutions that balance these objectives.

### 3.2 Methodology used

The model which is numerically investigated is reverse pump turbine with splitter blades in runner which has five main components: scroll casing, stay vanes, guide vanes, runner impeller and draft tube as shown in **Fig.3.1**. The number of blades in stay vanes, guide vanes and runner are 20,20 and 6. With the help of geometric design software CF turbo to create this Reverse Pump Turbine (RPT) model. The dimensions of the investigated RPT model are presented in the table below.

Table 1 Geometric parameters of RPT model

Parameters	Symbols	Values
Runner Specific Speed (min-1)	$nq$	36.8
Runner Inlet Dia. (mm)	$D_{ri}$	560
Runner Outlet Dia. (mm)	$D_{ro}$	270
Runner Blade Number (-)	$Z_r$	6
Guide Vane Distribution Dia. (mm)	$D_g$	662
Guide Vane Height (mm)	$B_g$	37.8
Guide Vane number (-)	$Z_g$	20
Stay Vane Number (-)	$Z_s$	20
Stay Vane In Dia. (mm)	$D_{si}$	763
Stay Vane Out Dia. (mm)	$D_{so}$	966

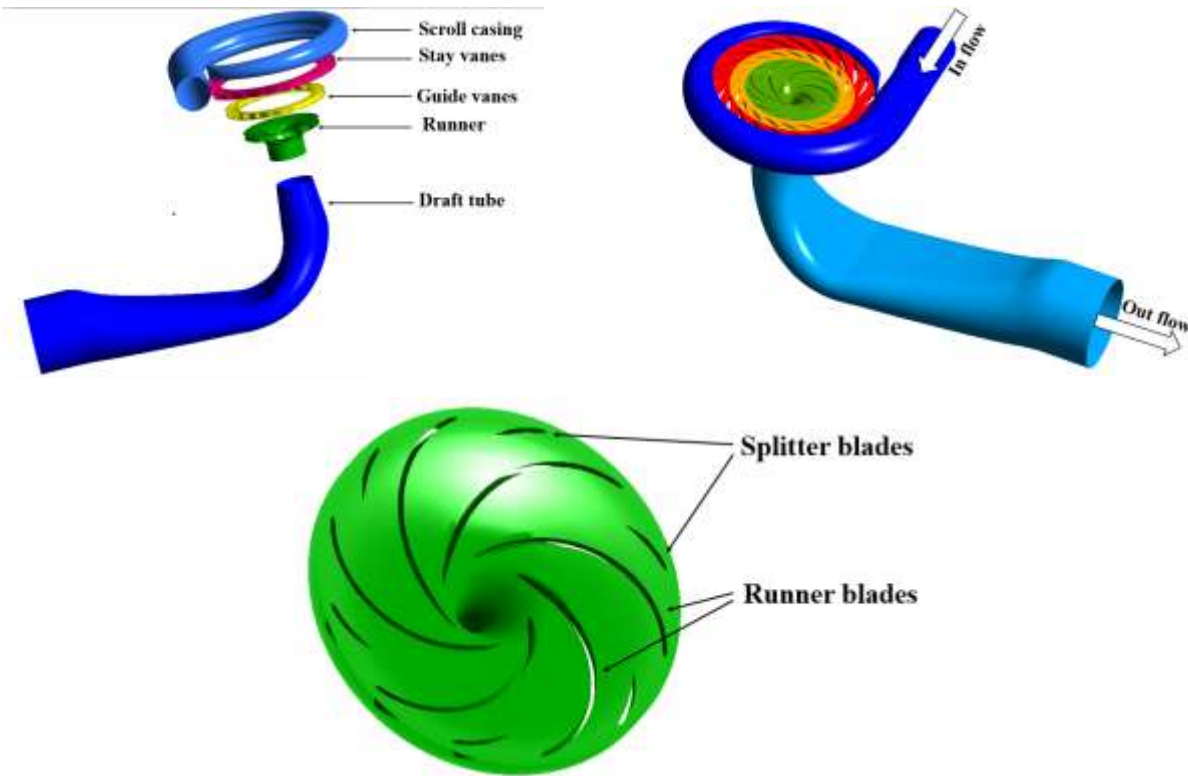
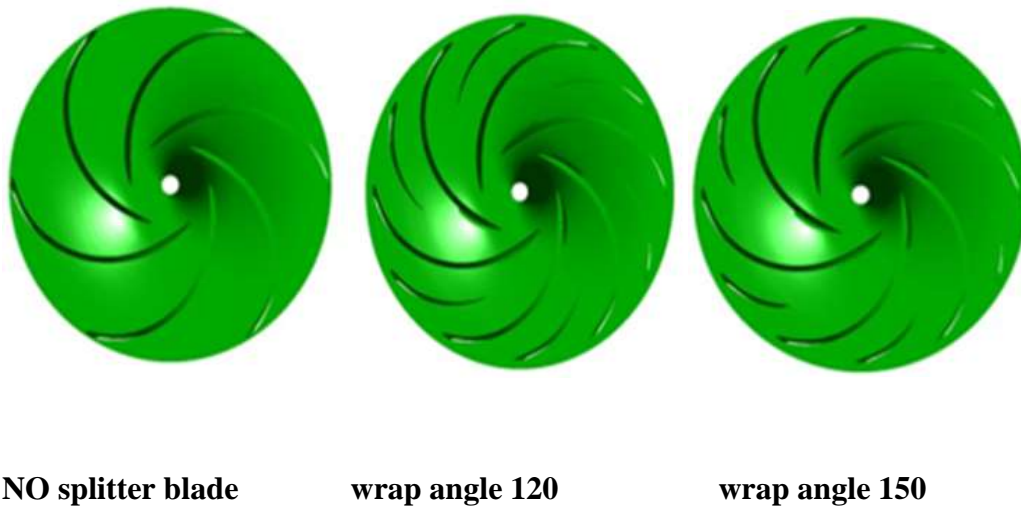


Figure 3-1:RPT Computational model and its component

All pf these operating was carried for the RPT model with runner having no splitter blade to visualize the condition that provide more flow instabilities, OP1 and OP11 were carried for both non-splitter blades RPT and other models with presence of splitter blades having different radius wrap angles WA1, WA2 and as it is revealed in **Fig.3.2** .



**NO splitter blade**

**wrap angle 120**

**wrap angle 150**

Figure 3-2 Runner with different wrap angle configuration

### 3.3 RPT Operation in Turbine Mode:

In turbine mode, high-pressure water enters the scroll casing inlet. It then flows through the stay vanes' and guide vanes' vaneless space before reaching the runner's inter-blade flow channels. Here, kinetic energy is converted into mechanical energy. Finally, the water exits through the draft tube outlet. This process is mirrored in the numerical simulation.

Guide vanes regulate water flow within the RPT. Their opening can vary from 1mm to 39mm depending on the desired power output. In this study, a 34mm guide vane opening (GVO) was used as the flow condition.

#### 3.3.1 Mesh Generation:

To achieve the numerical analysis goals, a computational mesh of the RPT model is crucial. Meshing software like ICM CFD and Turbo Grid was used to create meshes for all five components as they are presented in **Fig.3.3**. A structured hexahedral mesh was employed for the volute casing, stay vanes, guide vanes, and draft tube. The runner, however, utilized an unstructured hexahedral mesh. To precisely understand flow behavior near blades and vanes, particularly close to walls, a very fine mesh was used in these critical areas. This ensures the first layer of cells ( $y^+$ ) remains everywhere closer than a specific distance (typically around 30) from the wall.

Table 2 Grid details of RPT components

Component	Number of elements	Quality
Volute casing	314,327	0.5
Stay vane	352,260	0.65
Guide vane	820,040	0.67
Runner	3,875,961	0.34
Draft tube	1,115,730	0.7
Total mesh number	6,478,318	

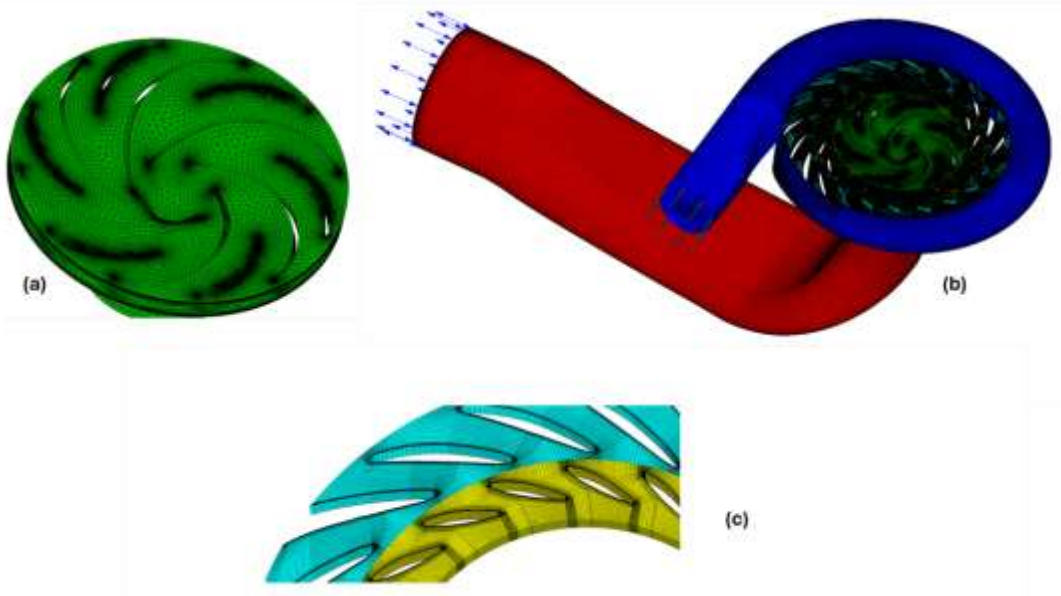


Figure 3-3 Grid generation for RPT Model components (a). runner (b). full RPT model (c). stay vane and guide vane

### 3.3.2 Numerical scheme

CFD simulations were conducted to analyze the flow instabilities in reverse pump turbine with the use of commercial ANSYS CFX 2019 Inc., ANSYS ICEM CFD and turbo grid were used for grid generation

Turbulent model as an important factor in CFD simulation, a Mentor's Shear Stress Transport turbulence model (SST) which is in Reynolds-Average Navier-Stocks (RANS) is used as it provides more accurate solutions to flow problems where it combines the advantages of both k-w and k-e model thus provides the analysis for both inner region boundary layer and shear flow in reverse pump turbine simulation.[48] The flow behavior was analyzed by adopting the conservation of mass (1),(2), momentum conservation equations (3) and SST equations (4),(5) having the following mathematical expression:

$$\frac{Dp}{Dt} + \rho(\nabla \cdot \vec{V}) = 0 \quad \dots (1)$$

$$\frac{\partial \rho}{\partial t} + \frac{\partial}{\partial x}(\rho u) + \frac{\partial}{\partial y}(\rho v) + \frac{\partial}{\partial z}(\rho w) = 0 \quad \dots (2)$$

$$\rho \frac{DV}{Dt} = \sigma g - \nabla P + \mu \nabla^2 V = 0 \quad \dots (3)$$

$$\frac{\partial(\rho k)}{\partial t} + \frac{\partial(\rho u_j k)}{\partial x_j} = P - \beta^* \rho \omega k + \frac{\partial}{\partial x_j} \left[ (u + \sigma_k \mu_t) \frac{\partial k}{\partial x_j} \right] \quad \dots (4)$$

$$\frac{\partial(\rho \omega)}{\partial t} + \frac{\partial(\rho u_j \omega)}{\partial x_j} = \frac{\gamma}{v_t} P - \beta \rho \omega^2 + \frac{\partial}{\partial x_j} \left[ (u + \sigma_\omega \mu_t) \frac{\partial \omega}{\partial x_j} \right] + 2(1 - F_1) \frac{\rho \sigma_\omega}{\omega} \frac{\partial k}{\partial x_j} \frac{\partial \omega}{\partial x_j} \quad \dots (5)$$

Numerical simulation process involves the simulation of RPT model for different operation points (OPs) as steady state simulation which provides result file which must serve as initial state of transient simulation. For single experimented guide vane opening of 34 mm was used. Five operating points we selected from experimental S-shape characteristic curve (OP1, OP5, OP11 and OP15) where each have the boundary conditions. For numerical simulations boundary conditions were taken as inlet mass flowrate and outlet static pressure corresponding to those operating points

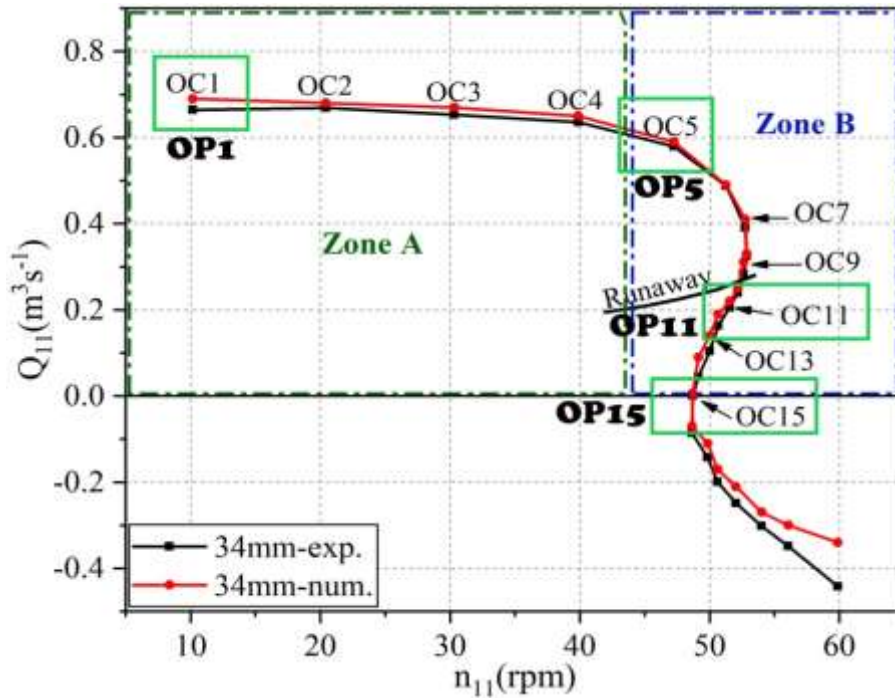


Figure 3-4, Comparison of numerical and experimental Discharge-Speed ( $Q_{11}$ - $n_{11}$ ) curve

To assess the accuracy of the chosen simulation approach, the numerically obtained **characteristic curves** for dimensionless flow rate ( $Q_{11}$ ) versus dimensionless rotational speed ( $N_{11}$ ) were compared to experimental data (**Fig.3.4**). The global error between the numerical and experimental results was found to be less than 4%, indicating a high degree of agreement and confidence in the utilized numerical scheme and its predictions.

The mathematical expressions for the dimensionless rotational speed ( $N_{11}$ ) and dimensionless flow rate ( $Q_{11}$ ), are presented in Equations (6) and (7), respectively[9]

$$n_{11} = \frac{nD1}{\sqrt{H}} \quad \dots (6)$$

$$Q_{11} = \frac{Q}{D_{11}^2 \sqrt{H}} \quad \dots (7)$$

*Table 3: Details of selected operating points*

Operating points	Flow coefficient ( $Q_{11}$ )	Speed coefficient ( $n_{11}$ )	Operating zone
OP 1	0.664269	10.166348	Turbine
OP 5	0.579705	47.254189	Turbine
OP 11	0.205483	51.54634	Turbine brake
OP 15	0.00129	48.690881	Turbine brake

# Chapter4 RESULT DISCUSSION

## 4.1 Velocity streamlines characteristics and analysis

For the two analyzed flow operating point and two different splitted blade wrap angles, a stream wise plane intersecting the stay/guide vanes and runner flow passages at mid-channel height ( $z/H = 0.5$ ) was chosen to investigate the internal flow dynamics and potential structural changes within the reversible pump turbine components (see **Fig.4.1**). This plane represents the average flow behavior across the blade span, where H represents the total distance between the hub and shroud. Figure 8 further clarifies the positions of the stay/guide vanes, vaneless space, and runner blades within this mid-span plane.

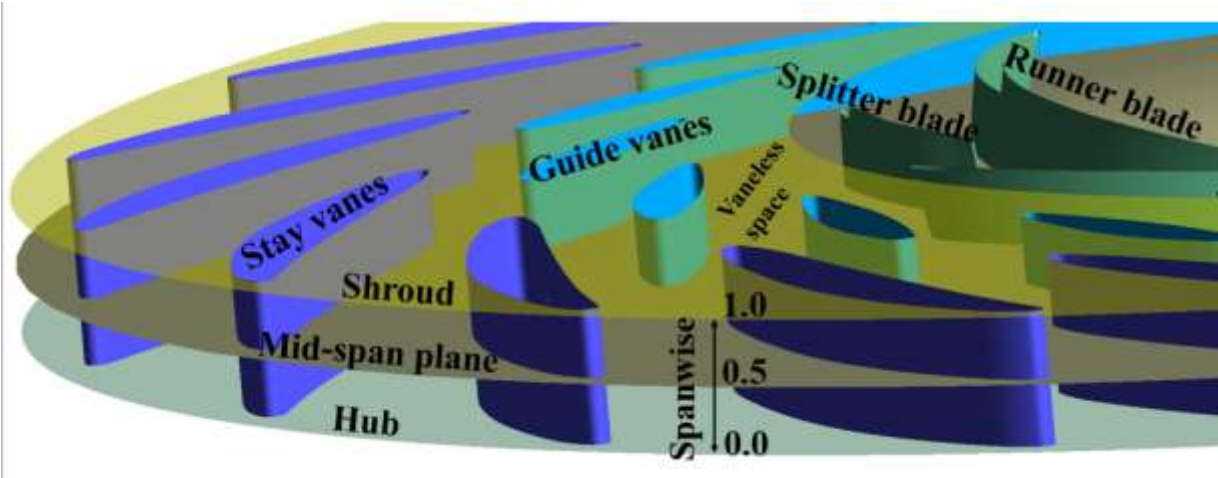


Figure 4-1 Mid-span plane presentation

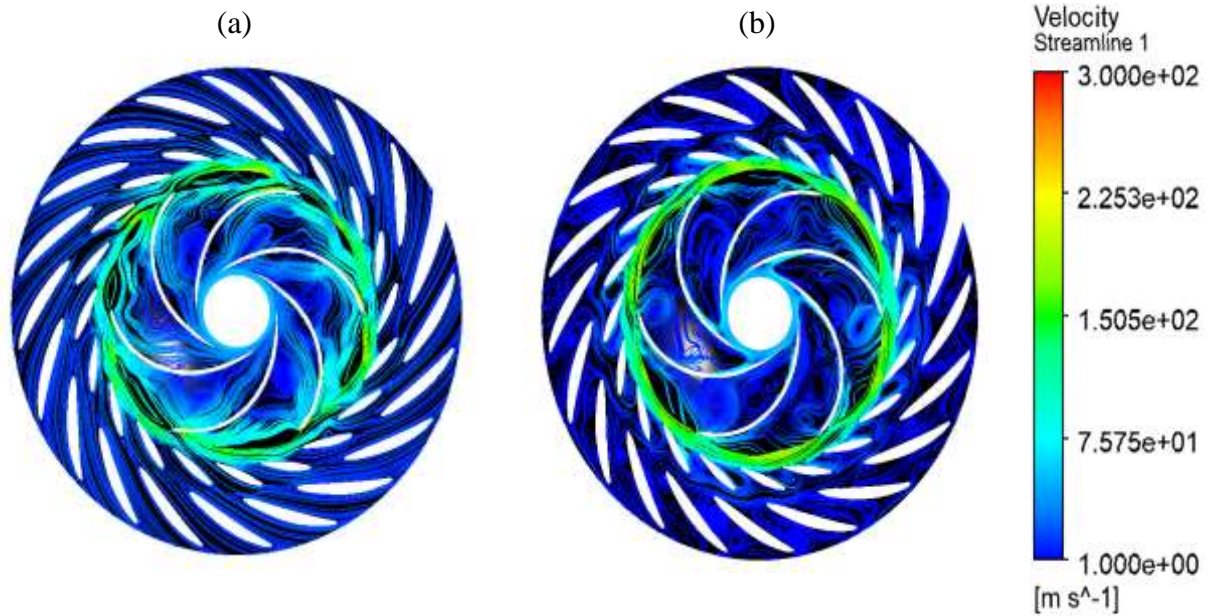


Figure 4-2: Velocity streamlines within RPT turbo-component stay vane, guide vane and runner inter-blade flow channel without inclusion of splitter blades at different operating point

(a). OP8 (b). OP9

The analysis of velocity streamlines (**Fig.4.2**) and velocity curl figures (**Fig.4.3**) provides valuable insights into flow instabilities within the reverse pump turbine operating in turbine mode for different operating points (OP). Where OP8 and OP9 both operating points exhibit well-distributed streamlines in the stay vanes and guide vanes, indicating smooth flow through these components. However, significant flow separation occurs at the runner inlet for both points. This separation leads to backflow and vortices forming in the vaneless space of the runner. OP9 appears to experience more severe flow separation compared to OP8, suggesting a more significant instability at this operating point. **Fig.4.3** confirms this with high vorticity concentrated in the runner for OP9 and between the guide vanes and runner inlet for OP9.

OP5 operating point demonstrates the most desirable flow behavior. Streamlines are well-distributed across all turbine components (stay vanes, guide vanes, and runner) with no signs of flow separation in **Fig.4.2**. This is further supported by the absence of excessive vorticity in **Fig.4.3**. This suggests stable and efficient flow through the turbine at OP5. And OP15 the operating

point exhibits the most significant flow instability. Backflow cells and vortices are prevalent throughout all components (stay vanes, guide vanes, and runner) as shown by the disrupted streamlines in **Fig.4.2**. The high vorticity throughout the turbine in **Fig.4.3** further confirms this observation. This suggests a highly unstable flow condition at OP15, which is less compared to the vorticity I OP9

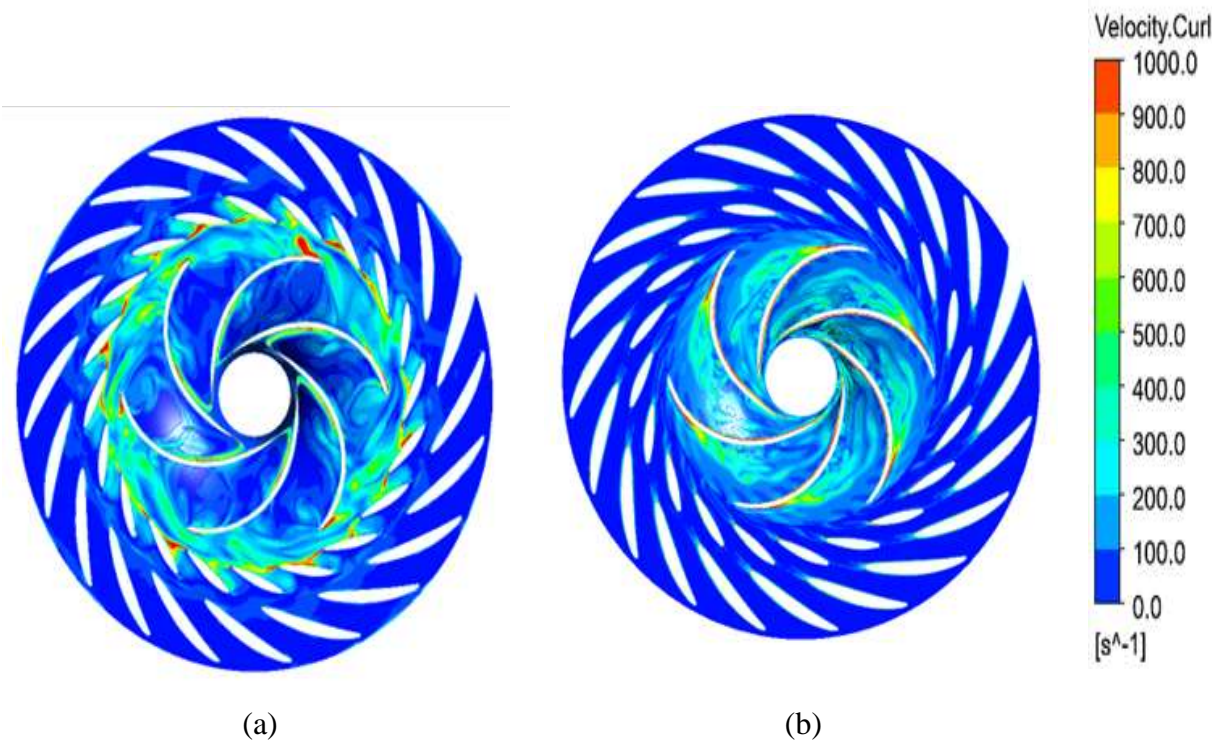


*Figure 4-3: Evolution of velocity curl within RPT turbo-component stay vane, guide vane and runner inter-blade flow channel without inclusion of splitter blades at different operating point (a). OP8 (b). OP9*

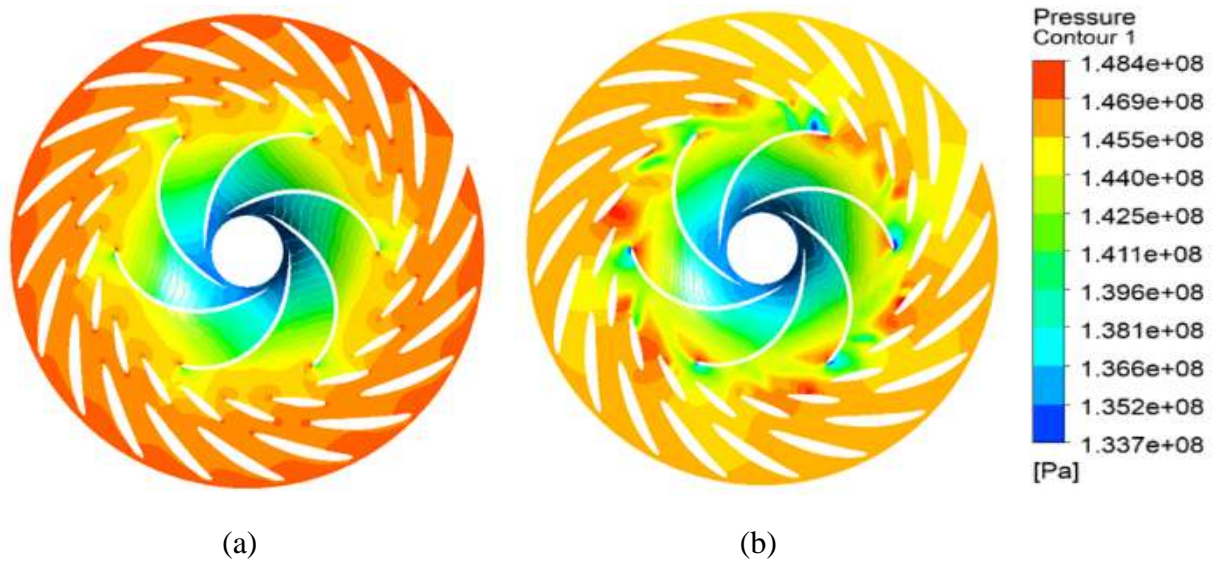


*Figure 4-4: Pressure contours within RPT turbo-component stay vane, guide vane and runner inter-blade flow channel without inclusion of splitter blades at different operating point*

(a). OP8 (b). OP9

pressure contours in the vaneless space of the stay vane, guide vane, and runner flow channel for the reverse pump turbine under different operating points OP8, OP9, is shown in **Fig.4.4**, where the pressure distribution in a reverse pump turbine varies depending on the operating point. At low flow conditions (OP8), pressure losses are high due to recirculation zones. As flow increases (OP9), the pump efficiency improves, leading to a slight pressure rise. The pressure reaches its maximum at the peak efficiency point (OP9). Further increase in flow beyond the optimal capacity results in pressure reduction due to inefficiencies.

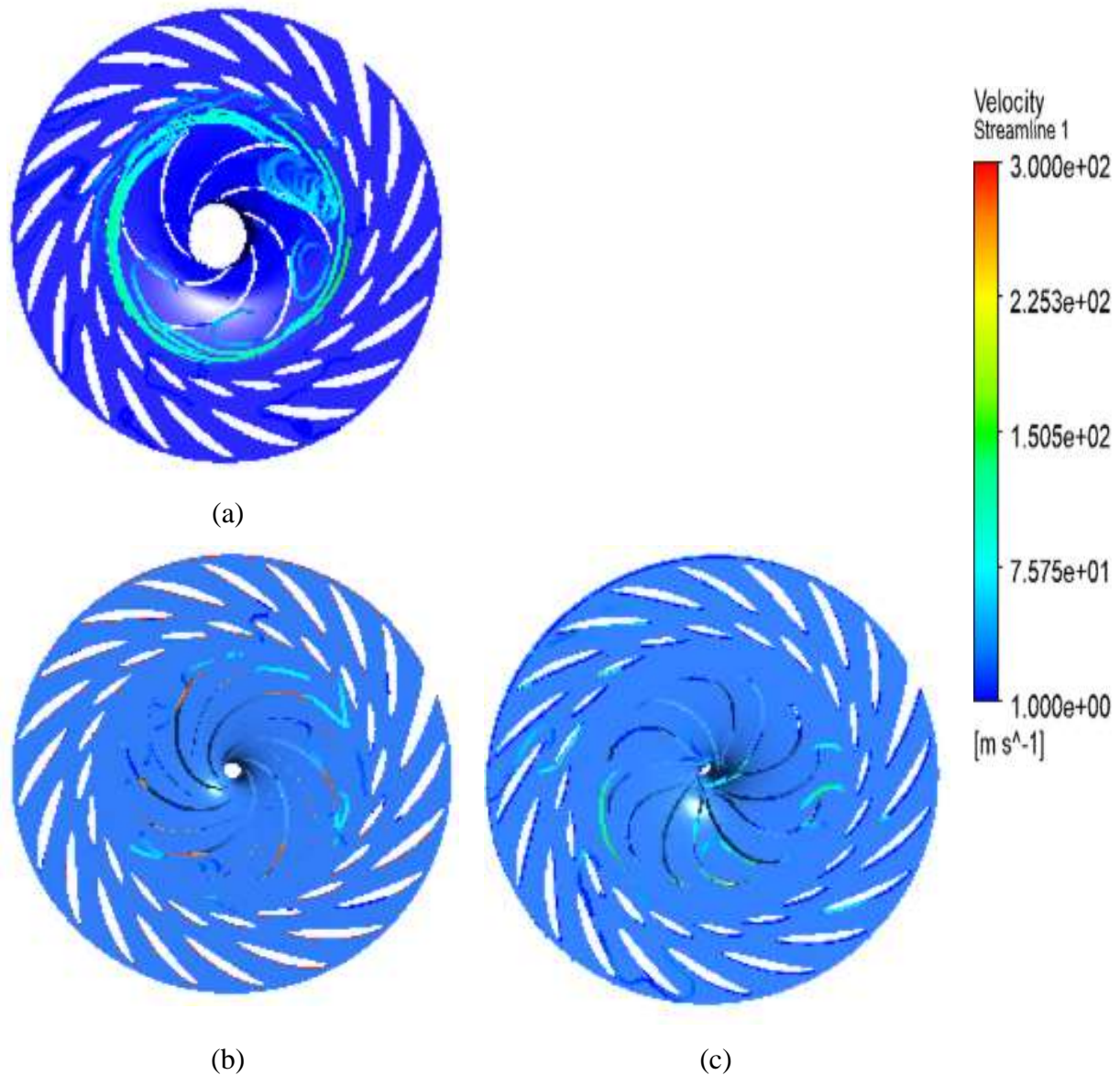


Figure 4-5: Velocity streamlines within RPT turbo-component stay vane, guide vane and runner inter-blade flow channel of operating point of OP 8 at different wrap angle of blades (a). No splitter (b). WA1 (c). WA2 (c).

At low flow rates (OP8), reverse pump turbines are particularly susceptible to flow separation. The introduction of splitter blades within the runner serves as a strategic intervention to address flow separation at OP8. These blades effectively divide the flow passage into smaller channels, influencing the velocity distribution and mitigating separation. It is observed that the absence of splitter blades allows for a wider, unobstructed flow path. However, this configuration struggles to maintain attached flow at OP8. In **Fig.4.5**, the streamlines

exhibit significant deviations from the intended path, indicating regions of separation. These separated flows can create backflow cells and contribute to increased vorticity (turbulence).

While the presence of splitter blades alters the flow pattern. The streamlines become more constrained and follow a more defined path along the runner blades. This indicates a significant reduction in flow separation compared to the no-splitter case.

It is observed that bigger wrap angle of blades provide a more pronounced channeling effect, further reducing flow separation and minimizing the formation of backflow cells. Conversely, smaller wrap angle offer less flow guidance, resulting in a higher degree of vorticity compared to bigger wrap angle. In addition, it is observed in **Fig.4.6**, where the introduction of splitter blade results in increase in velocity curl, which is reduced as the wrap angle, is increased.

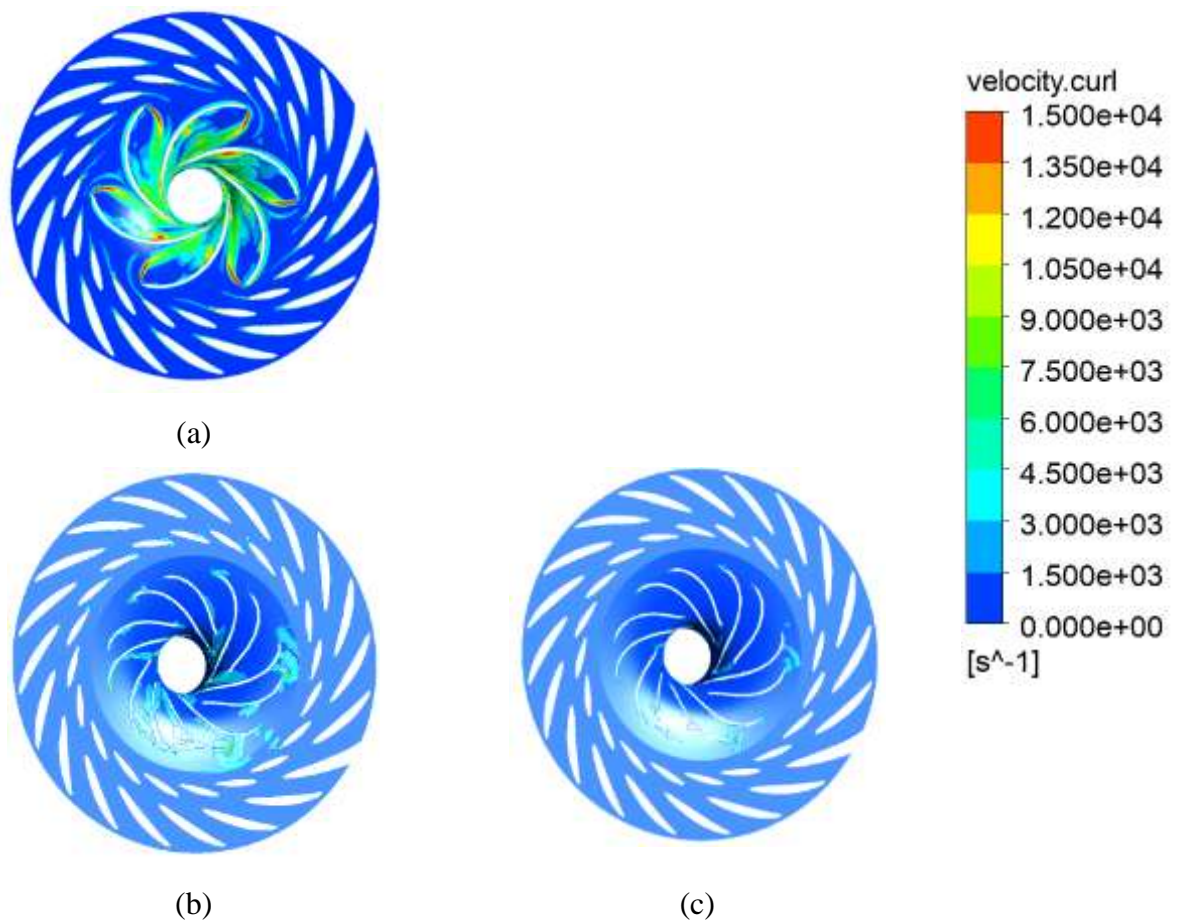
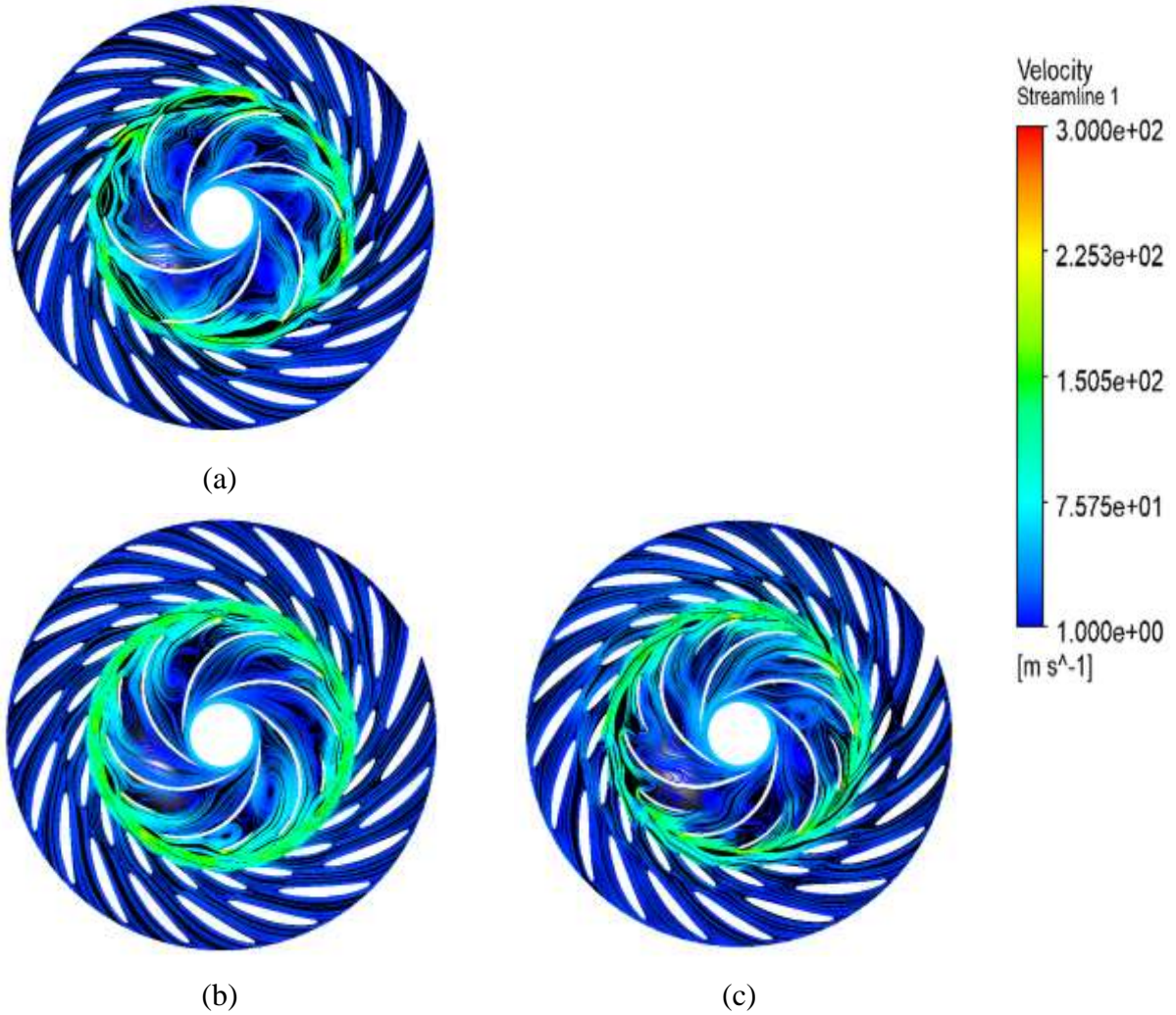


Figure 4-6: Evolution of velocity curl within RPT turbo-component stay vane, guide vane and runner inter-blade flow channel of operating point of OP 8 at different wrap angle of blades

(a). No splitter (b). WA1 (c). WA2



*Figure 4-7: Velocity streamlines within RPT turbo-component stay vane, guide vane and runner inter-blade flow channel of operating point of OP 9 at different wrap angle*

(a). No splitter (b). WA1 (c). WA2

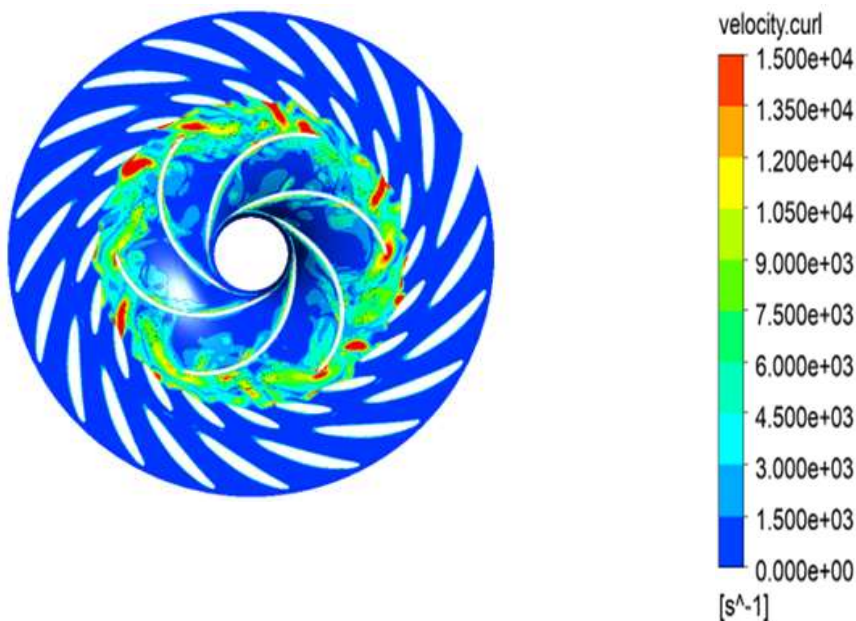
At OP9 in **Fig.4.7**, the turbine operates near its peak efficiency. However, without splitter blades, the flow struggles to follow the intended path through the runner blades. This results in **flow separation**, where the fluid detaches from the blade surface, leading to energy losses, increased turbulence and backflow cells formation.

### Impact of blade wrap angle on Splitter-Bladed Reversible Pump Turbines:

The biggest wrap angle (WA1) demonstrates the most significant reduction in flow separation and backflow formation. This translates to the most streamlined flow pattern and likely the highest efficiency among the configurations.

The smaller - wrap angle (WA2) shows some remaining flow separation compared to WA1. However, it still offers a substantial improvement over the no-splitter case.

In addition, in **Fig.4.8**, the analysis suggests that velocity curl (related to turbulence) are highest without a splitter blade and decrease with the introduction of splitter blades. This is consistent with the observed reduction in flow separation and turbulence. As the splitter wrap angle is reduced (WA2 to WA1), the velocity curl is observed to increase slightly, potentially indicating a minor rise in localized turbulence near the shorter blades.



(a)

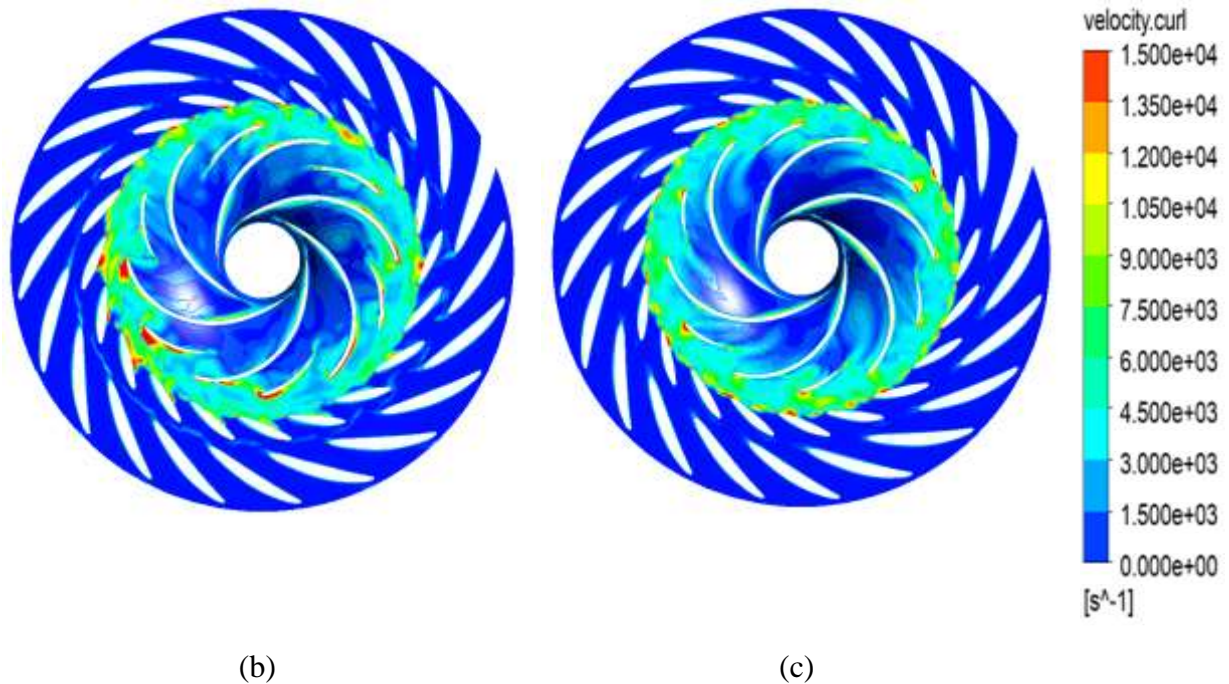
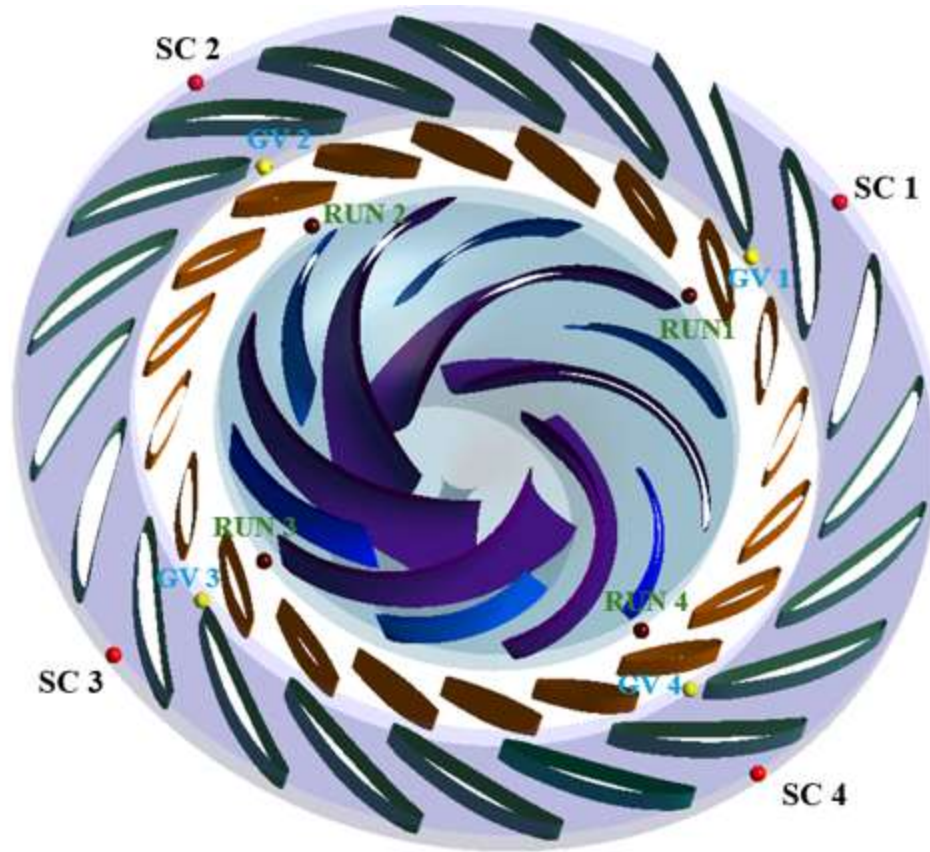


Figure 4-8: Evolution of velocity curl within RPT turbo-component stay vane, guide vane and runner inter-blade flow channel of operating point of OP 9 at different wrap angle

(a). No splitter (b). WA1 (c). WA2

## 4.2 Pressure pulsation characteristics and analysis

To elucidate the dynamic evolution of flow within the reversible pump turbine (RPT) and establish a clear correlation with the corresponding pressure pulsations at various flow regions, a comprehensive investigation into local pressure pulsation characteristics is undertaken. To achieve this, pressure monitoring points were strategically positioned at various flow zones within the RPT components' vaneless spaces. The investigation encompassed different wrap angle (WA1, WA2) and two operating conditions (OP8 and OP9).



*Figure 4-9 Position of pressure monitoring points at different flow zones (runner, guide vanes and stay vanes)*

The pressure distribution within the RPT was captured using a network of pressure monitoring points. These points were strategically placed to capture key flow characteristics as shown in **Fig.4.9**: Four monitoring points (SC1-SC4) were positioned within the scroll casing near the inlet zone of the stay vanes. This placement allows for measurement of the upstream pressure conditions impacting the stay vanes. And other four additional points (GV1-GV4) were located at the outlet of the stay vanes, which coincides with the inlet of the guide vanes. These points capture the pressure distribution after the flow exits the stay vanes and enters the guide vanes; also, four more points (RUN1-RUN4) were positioned within the runner inlet zone. Finally three point in the Draft tube. These points were spaced at constant angular intervals of  $90^\circ$  around the circumference. This configuration allows for the evaluation of circumferential pressure variations at the runner inlet.

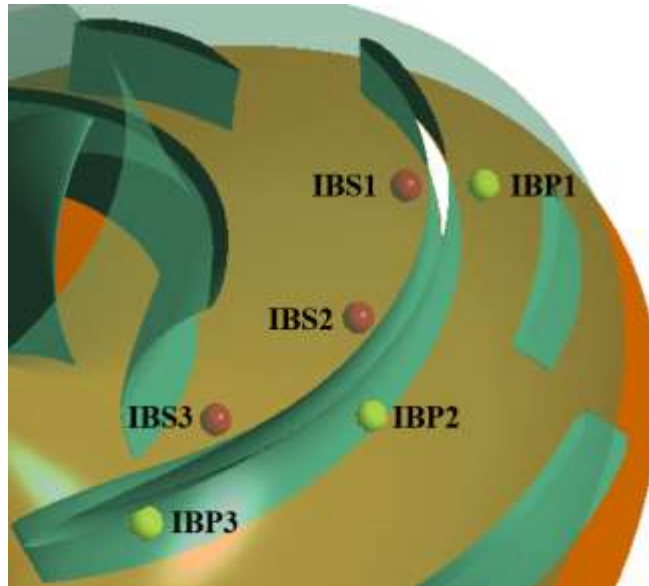
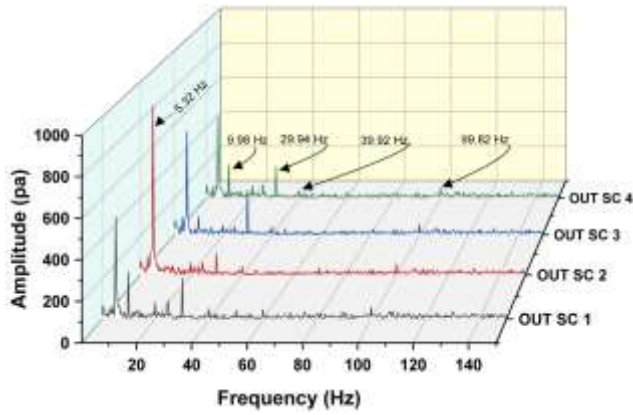
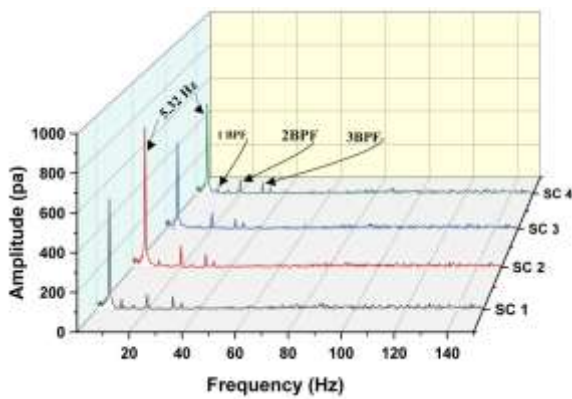


*Figure 4-10 Position of pressure monitoring points on runner inter-blade flow passage on suction and pressure sides of runner blade*

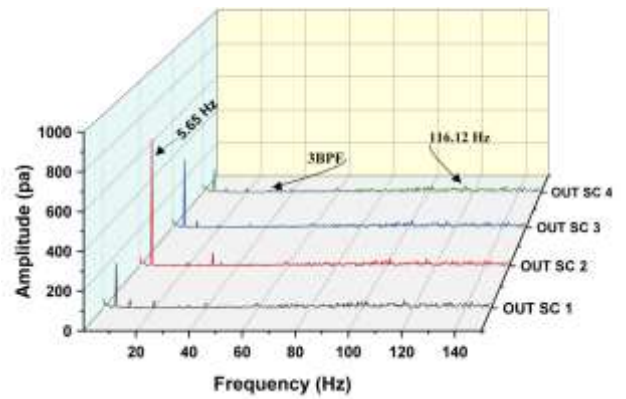
Focusing on the internal flow path within the runner blades (inter-blade flow zone), the analysis considered only a single runner blade. Three monitoring points were strategically positioned along the blade passage based on a unit streamwise distance (normalized distance) measured from the runner outlet to the runner inlet. Where IBS1, IBS2, and IBS3: Located on the suction side of the blade (the side where low pressure facilitates fluid acceleration). And IBP1, IBP2, and IBP3: Positioned on the pressure side of the blade (the side where high pressure exerts force on the blade) as shown in **Fig.4.10**.



(a)



(b)



(c)

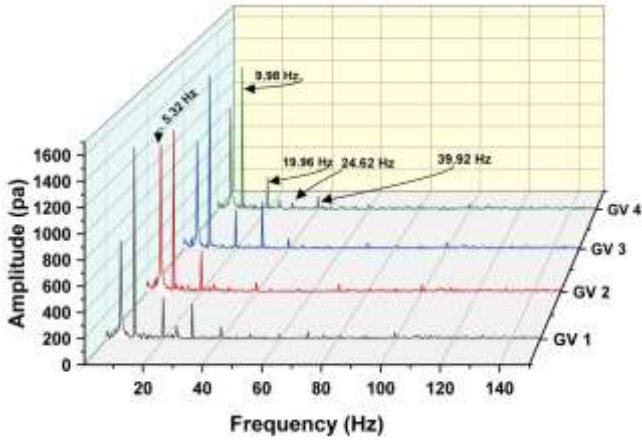
Figure 4-11: FFT-based frequency spectra of pressure pulsation within the vaneless space around the outlet of scroll casing with operating point 8(O8) at different wrap angle with splitter blades.

(a). No splitter (b). WA1 (c). WA2.

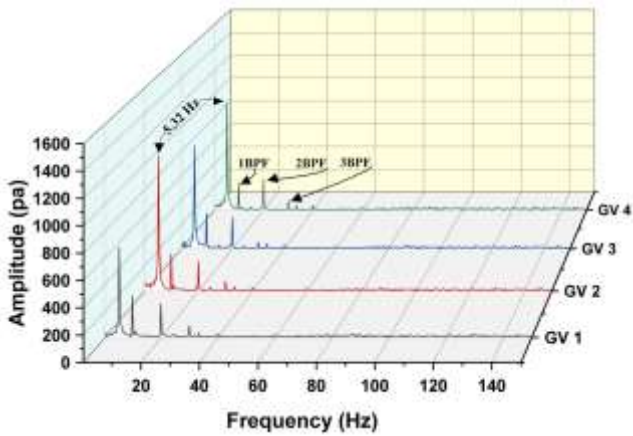
In **Fig.4.11**, the absence of splitter blades leads to a higher BPF compared to configurations with splitter blades. This suggests a more pronounced interaction between the runner and the scroll casing due to potentially increased flow separation and turbulence in the runner without splitters. The introduction of splitter blades with wrap angle promotes a smoother flow pattern within the runner. This reduces flow separation and turbulence, leading to a lower BPF and potentially less intense interaction between the runner and the casing.

As the wrap angle of the splitter blade increases, the BPF appears to rise slightly. This might indicate a minor increase in localized flow disturbances near the shorter blades, leading to a slightly stronger interaction with the casing per blade passage. The discussion also mentions the presence of additional, lower-amplitude dominant frequencies in the pressure spectra. These frequencies are

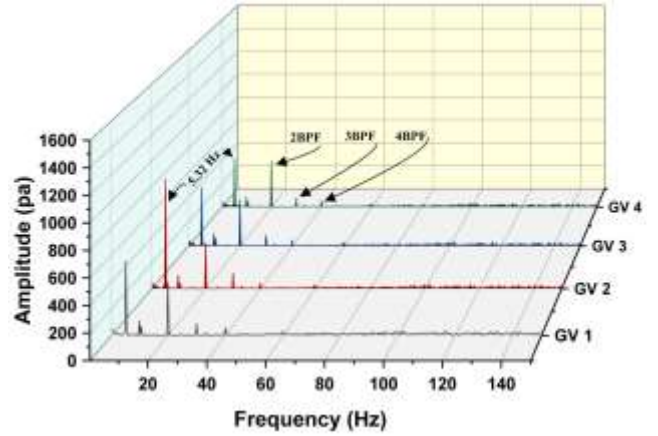
attributed to flow instabilities originating at the inlet of the stay vanes. The absence of splitter blades allows for more significant flow instabilities at the stay vane inlet, resulting in higher dominant frequencies associated with these instabilities. Similar to BPF reduction, splitter blades appear to mitigate flow instabilities at the the stay vane inlet. This translates to lower dominant frequencies in the pressure spectra related to these instabilities.



(a)



(b)



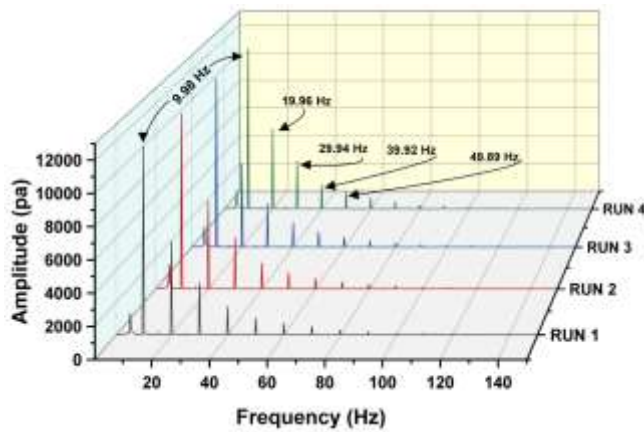
(c)

Figure 4-12: FFT-based frequency spectra of pressure pulsation within the vaneless space around the inlet of guide vanes with operating point 8(OP8) at different wrap angle with splitter blades (a). No splitter (b). WAI (c). WA2 (d).

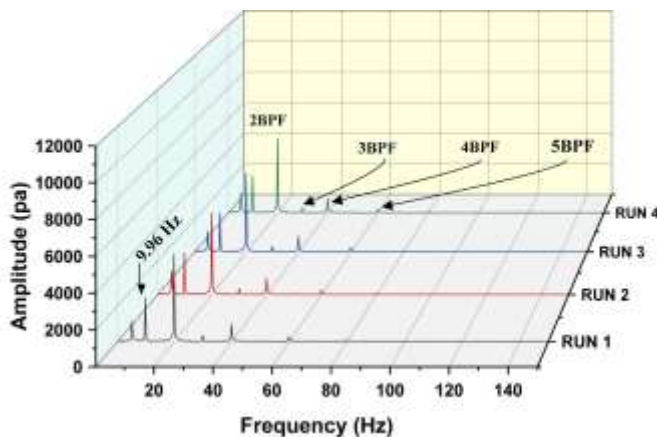
As shown in **Fig.4.12**, for the analysis of pressure pulsation between the stay vane outlet and the guide vane inlet demonstrates the influence of wrap angle with splitter blades on BPF reduction. The presence of additional frequencies suggests potential flow instabilities within the guide vanes. The higher BPF amplitude at the guide vane inlet compared to the stay vane outlet highlights the

potential influence of flow acceleration and guide vane geometry. This information can be valuable for optimizing both wrap angle with splitter blade design and guide vane geometry to achieve smoother flow and minimize pressure pulsations within the reverse pump turbine.

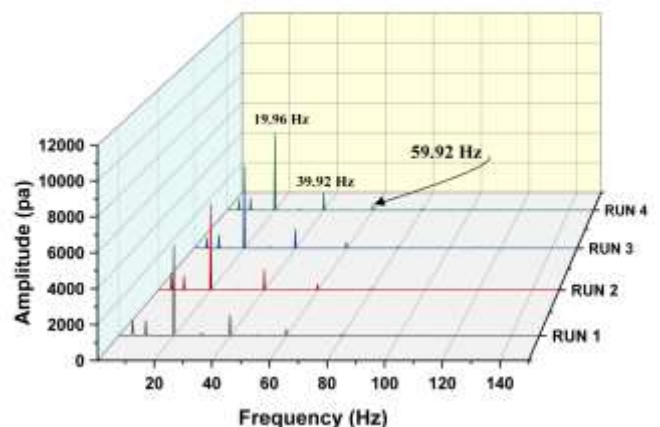
The analysis of pressure pulsation data at the runner inlet as shown in **Fig.4.13** reinforces the notion that wrap angle with splitter blades effectively reduce pressure pulsation. This reduction is primarily attributed to a lower Blade Passing Frequency (BPF) due to a smoother flow pattern within the runner with splitter blades. While the discussion acknowledges potential flow instabilities within the runner, the data suggests that these instabilities might not manifest significantly at the runner inlet location for the configurations analyzed. The overall takeaway is that splitter blades play a crucial role in promoting a more stable flow interaction between the runner and surrounding components within the reverse pump turbine.



(a)

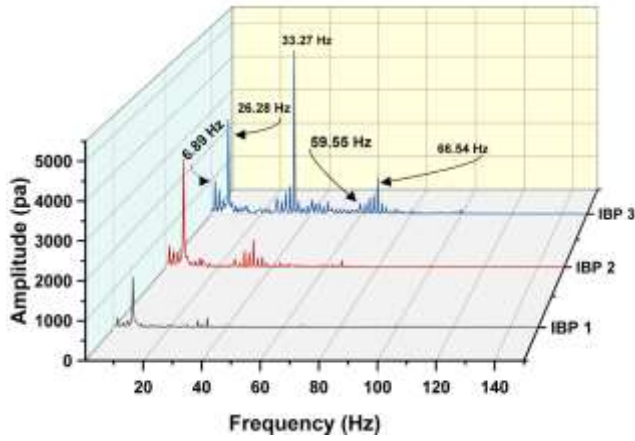


(b)

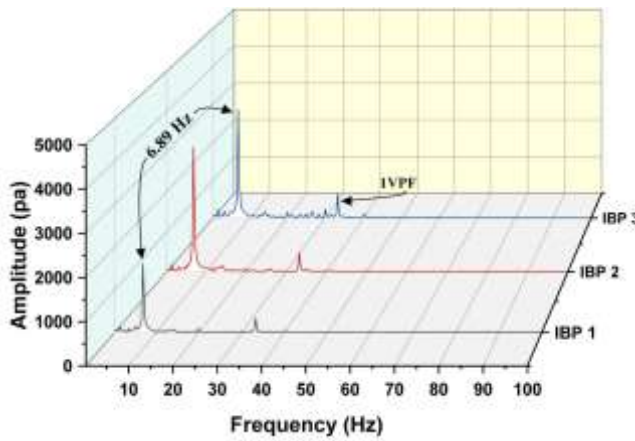


(c)

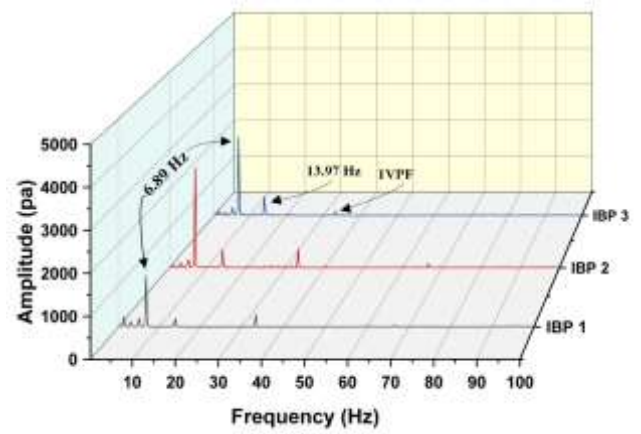
Figure 4-13: FFT-based frequency spectra of pressure pulsation within the vaneless space around the inlet of runner with operating point 8 (OP8) at different wrap angle with splitter blades (a). No splitter (b). WA1 (c). WA2 (d).



(a)



(b)



(c)

Figure 4-14: FFT-based frequency spectra of pressure pulsation within the runner inter-blade flow passage at pressure side of the runner with operating point 8 (OP8) at different wrap angle with splitter blades (a). No splitter (b). WA1 (c). WA2.

**Fig.4.14**, presents a detailed analysis of pressure pulsation within the inter-blade flow channels of a reverse pump turbine runner, focusing on the pressure side. Three monitoring points, IBP3 (inlet) to IBP1 (outlet), capture data analyzed using FFT to identify dominant frequencies

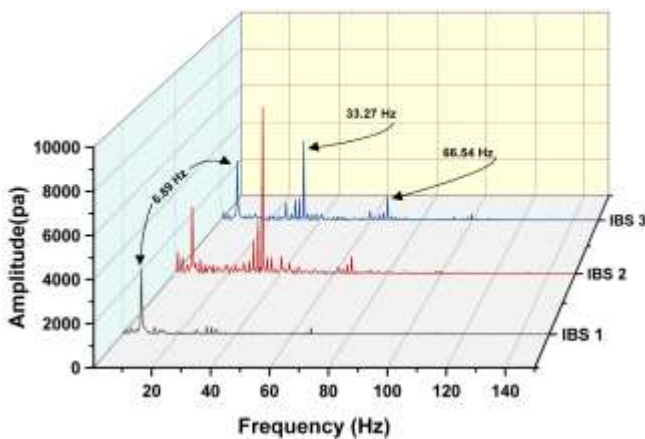
The absence of splitter blades leads to a significantly higher VPF amplitude across all monitoring points (IBP3 to IBP1). This suggests a more intense interaction between the guide vanes and the runner blades, potentially due to increased flow separation and turbulence within the runner without splitters. While the introduction of splitter blades promotes a smoother flow pattern within

the runner. This reduces flow separation and turbulence, leading to a lower VPF amplitude across all monitoring points compared to the no-splitter case.

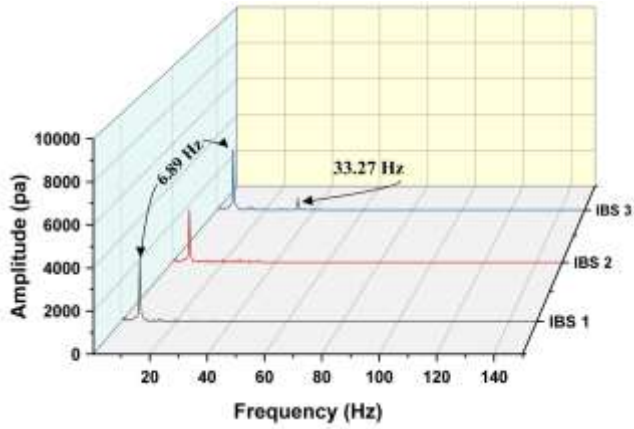
As the wrap angle with splitter blade increases (WA1 to WA2), the VPF amplitude shows a slight upward trend across the monitoring points. This suggests a minor rise in localized flow disturbances near the shorter blades, potentially leading to a slightly stronger interaction between the vanes and blades. Interestingly, the VPF amplitude appears to increase slightly as the flow progresses from IBP3 (inlet) to IBP1 (outlet) in all configurations. This could be attributed to the cumulative effect of multiple vane passages and potential interactions with the diffuser at the outlet.

While VPF is the dominant frequency, the discussion acknowledges the presence of additional, lower-amplitude frequencies (Figure 11a). These are attributed to flow instabilities within the runner. The absence of splitter blades allows for more significant flow instabilities within the runner, resulting in higher-amplitude frequencies associated with these instabilities. Similar to VPF reduction, splitter blades appear to mitigate flow instabilities within the runner. This translates to lower-amplitude frequencies in the spectra related to these instabilities.

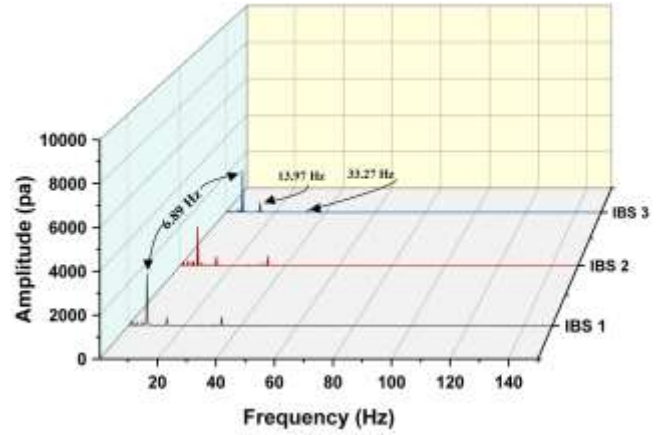
The discussion briefly mentions that a similar analysis was conducted for the runner's suction side in **Fig.4.15**. The results reveal the same trend for VPF with splitter blades (reduced amplitude compared to no-splitter) but with a generally lower overall amplitude compared to the pressure side. This suggests a less pronounced interaction between the vanes and blades on the suction side.



(a)

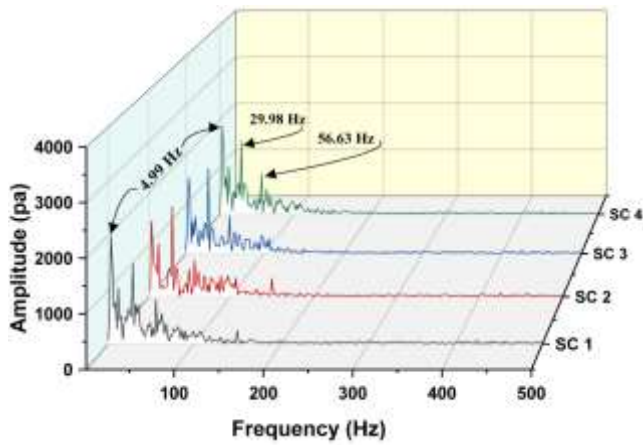


(b)

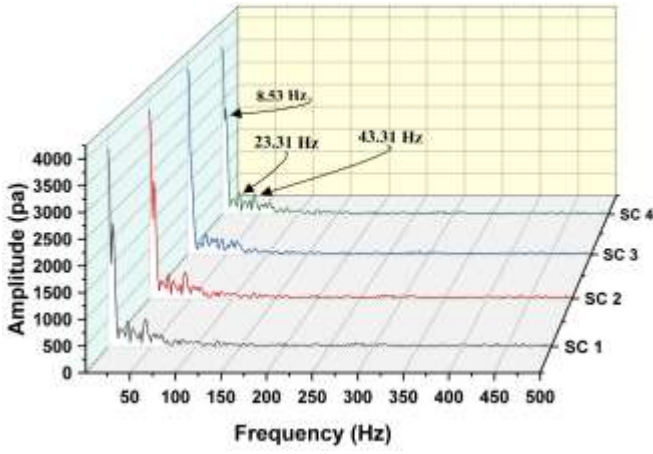


(c)

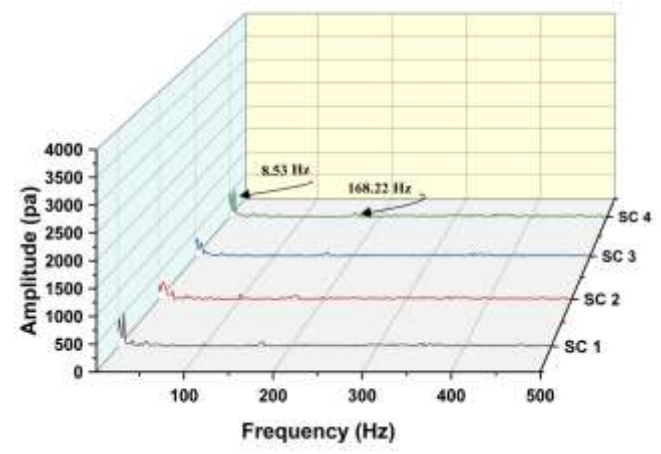
Figure 4-15: FFT-based frequency spectra of pressure pulsation within the runner inter-blade flow passage at suction side of the runner with operating point 8 (OP8) at different wrap angle with splitter blades (a). No splitter (b). WAI (c). WA2



(a)



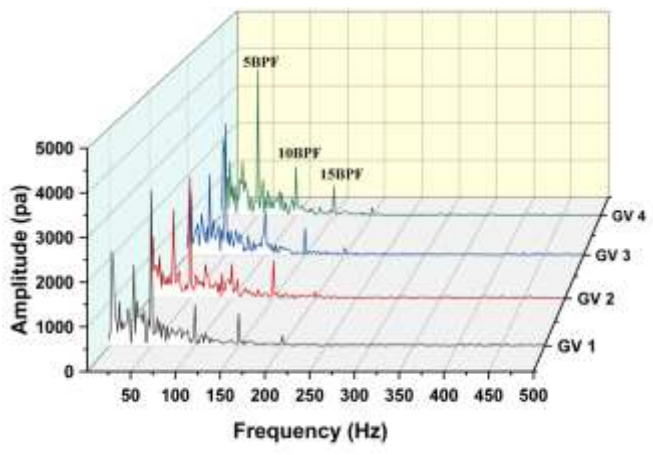
(b)



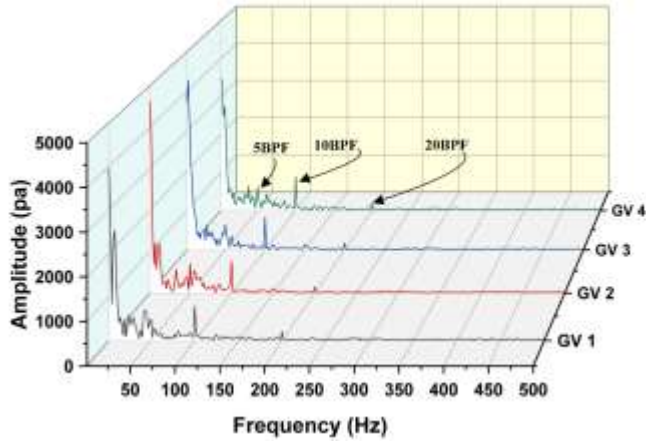
(c)

Figure 4-16: FFT-based frequency spectra of pressure pulsation within the vaneless space around the outlet of scroll casing with operating point 9 (OP9) at different wrap angle with splitter blades (a). No splitter (b). WA1 (c). WA2.

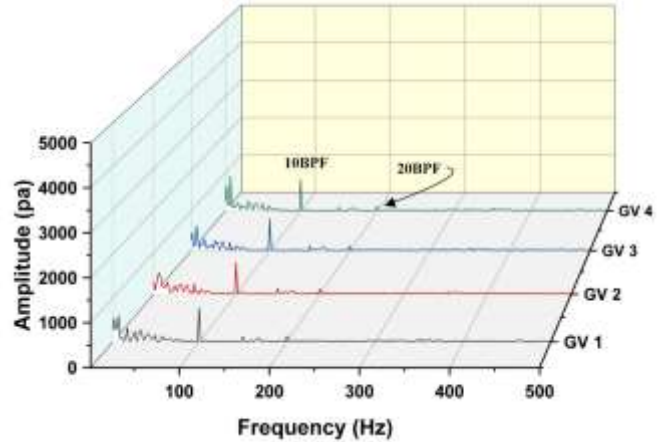
In **Fig.4.16**, there is existence of two dominant frequencies that are present: High Amplitude and low amplitude frequencies. A high-amplitude dominant frequency likely corresponds to flow instabilities within the stay vanes. A lower-amplitude dominant frequency is likely related to the blade passing frequency (BPF). Without splitter blades, both dominant frequencies (instability and BPF) exhibit higher amplitudes, suggesting significant flow disturbances and blade interaction. With splitter blades: The introduction of wrap angle with splitter blades reduces the amplitude of both dominant frequencies. This indicates mitigated flow instabilities and potentially smoother blade passage. Bigger wrap angle with splitter blades might result in slightly lower instability and have higher BPF frequencies compared to longer ones.



(a)



(b)



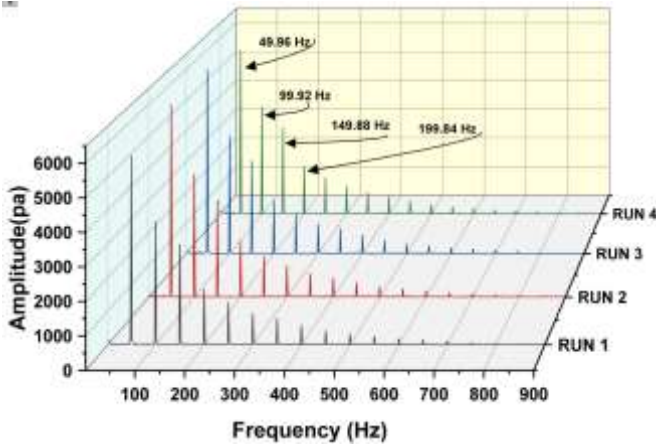
(c)

Figure 4-17: FFT-based frequency spectra of pressure pulsation within the vaneless space around the inlet of guide vanes with operating point 9 (OP9) at different wrap angle with splitter blades (a). No splitter (b). WA1(c). WA2.

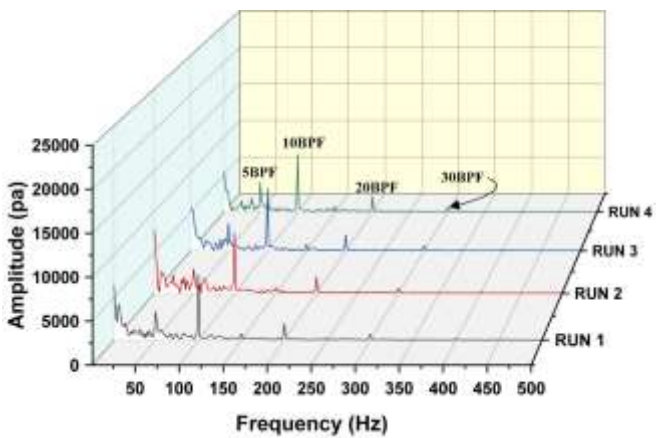
In **Fig.4.17**, the discussion emphasizes the presence of dominant frequencies in the spectra that are attributed to flow instabilities rather than Blade Passing Frequency (BPF). These instabilities likely originate upstream of the guide vanes and potentially intensify as the flow progresses through them.

The key observation is that the amplitude of these instability frequencies is significantly reduced with the introduction of wrap angle with splitter blades compared to the no-splitter case. The bigger wrap angle with splitter blade (WA 2) might achieve the most significant reduction in instability frequency amplitude based on **Fig.4.17. b** This aligns with the concept that shorter blades provide better flow guidance and promote a smoother flow path, potentially leading to the most effective reduction in upstream instabilities. The bigger- wrap angle with splitter blade (WA2) might exhibit a slightly higher instability frequency amplitude compared to WA1 but still significantly lower than the no-splitter case.

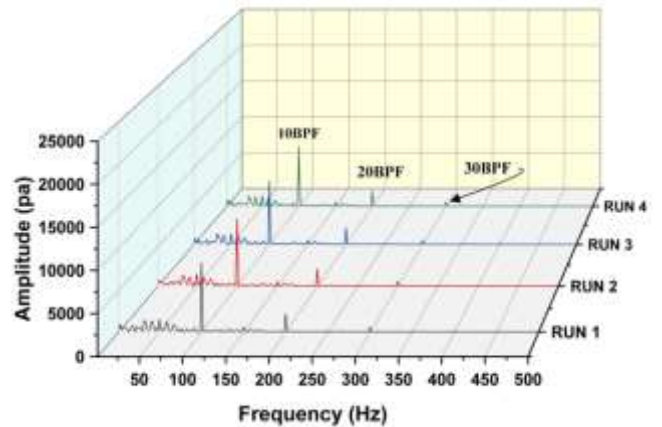
The smaller wrap angle with splitter blades exhibit the small existence of frequencies related to flow instabilities compared to other bigger wrap angle with splitter blades



(a)



(b)



(c)

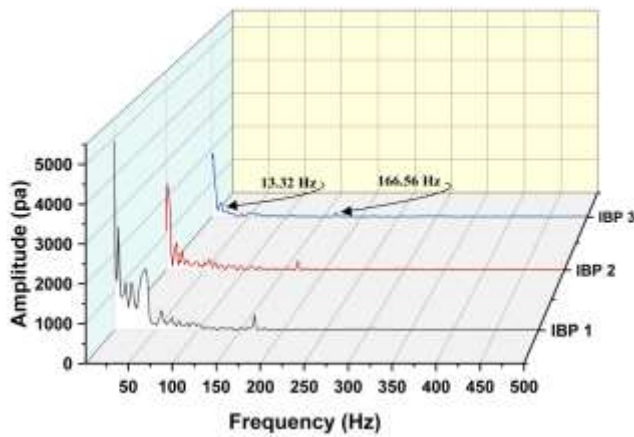
Figure 4-18: FFT-based frequency spectra of pressure pulsation within the vaneless space around the inlet of runner with operating point 1(OP11) at different wrap angle with splitter blades (a). No splitter (b). WA1 (c). WA2.

At the runner inlet using Fast Fourier Transform (FFT). The analysis is likely based on 15, which presumably showcases the pressure pulsation spectra for configurations with and without splitter blades, the absence of splitter blades leads to a significantly higher BPF amplitude in **Fig.4.18. a**. This suggests a more intense interaction between the runner blades and guide vanes, potentially due to increased flow separation and turbulence within the runner.

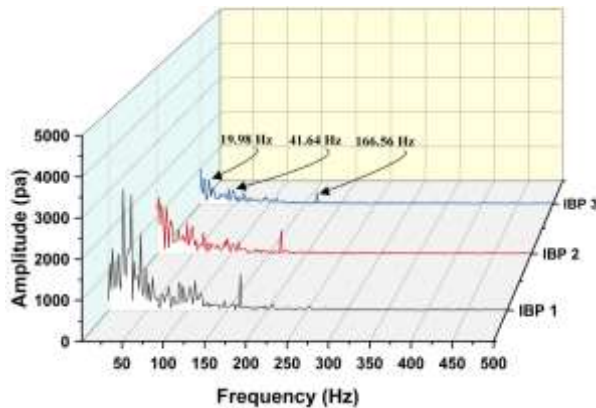
The introduction of wrap angle with splitter blades promotes a smoother flow pattern within the runner. This reduces flow separation and turbulence, leading to a lower BPF amplitude compared to the no-splitter case. As the wrap angle with splitter blade increases (WA1 to WA2), there might be a minor upward trend in BPF amplitude. This suggests a potential correlation between shorter

blades and slightly stronger blade interaction, possibly due to localized flow disturbances near the shorter blades.

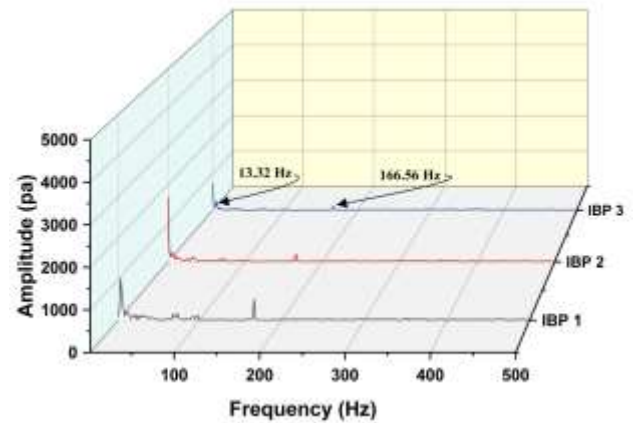
While BPF is the dominant frequency, the discussion acknowledges the presence of additional, lower-amplitude frequencies in the spectra. These frequencies are attributed to flow instabilities originating within the runner as it is observed that they exist with the presence of splitter blades due to the amplitude of dominant frequency related to BPF are reduced and these frequencies are reduced as we have bigger wrap angle with splitter blades.



(a)



(b)



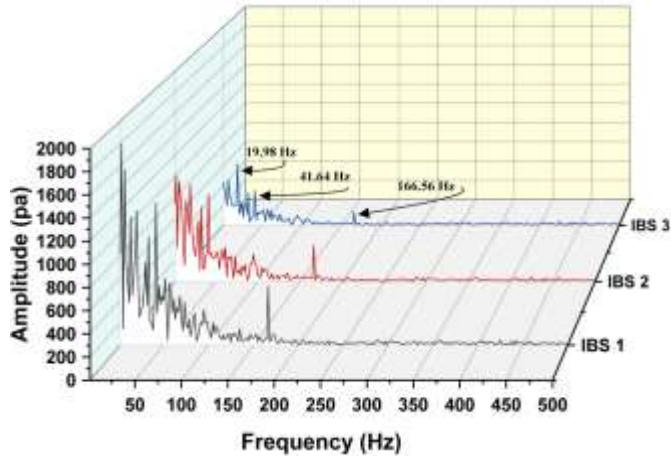
(c)

Figure 4-19: FFT-based frequency spectra of pressure pulsation within the runner inter-blade flow passage at pressure side of the runner with operating point 9 (OP9) at different wrap angle with splitter blades (a). No splitter (b). WA1(c). WA2.

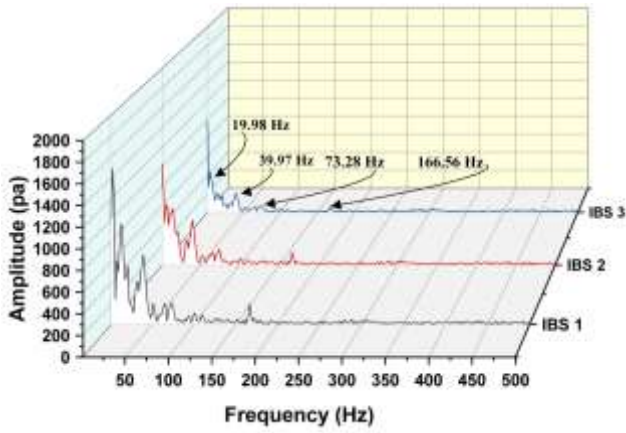
In **Fig.4.19**, the absence of splitter blades, the spectra exhibit high-amplitude dominant frequencies. These frequencies are attributed to flow instabilities occurring within the runner. These instabilities likely disrupt the smooth flow path and contribute to inefficiencies. Lower-amplitude dominant frequencies are also present, potentially corresponding to the Vane Passing Frequency (VPF). This signifies the interaction between the guide vanes and the runner blades as the blade passes each vane channel.

With the presence of wrap angle with splitter blades. There is notable reduction in the amplitude of dominant frequencies associated with flow instabilities. This suggests that splitter blades promote a smoother flow pattern within the runner, effectively mitigating these instabilities. While instability frequencies are reduced, VPF frequencies remain present in the spectra. However, the discussion highlights that the amplitude of these VPF frequencies exhibits a trend as the wrap angle with splitter blade increases (WA1 to WA2), the VPF amplitude tends to decrease. This suggests a potential correlation between bigger wrap angle with splitter blades and a smaller interaction between the guide vanes and runner blades, leading to a slightly lower VPF.

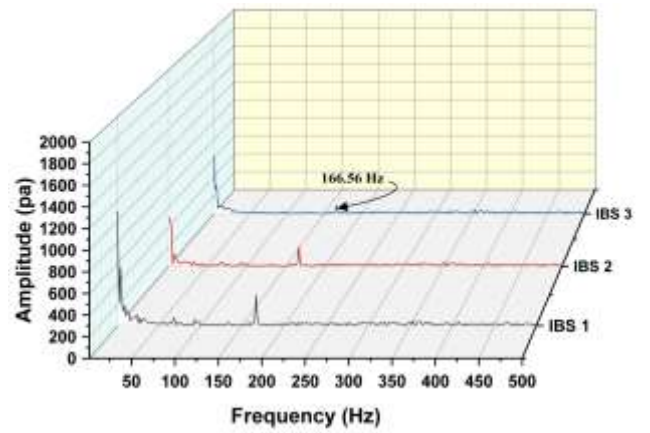
The discussion might acknowledge that the analysis was conducted for both the pressure side in Figure 16 and suction side of the runner as shown in **Fig.4.12**. While the overall trends regarding instability frequencies and VPF likely hold true for both sides, the specific amplitude values might differ. The pressure side typically experiences higher flow interaction forces compared to the suction side, potentially leading to slightly different dominant frequency amplitudes



(a)



(b)



(c)

Figure 4-20: FFT-based frequency spectra of pressure pulsation within the runner inter-blade flow passage at suction side of the runner with operating point 9 (OP9) at different wrap angle with splitter blades (a). No splitter (b). WA1 (c). WA2.

## Chapter5 Conclusion

This study focuses on the impact of vaneless space flow instability within a Reverse Pump Turbine (RPT) operating with a large Guide Vane Opening (GVO) of 34mm with presence wrap angle with splitter blades. A comprehensive investigation was conducted, considering the combined effects of flow conditions (analyzed at two operating points) and runner configurations with varying wrap angle with splitter blades (3 different wrap angle with splitter blades). Utilizing Computational Fluid Dynamics (CFD) simulations, the analysis encompassed these diverse operating scenarios. The key findings and conclusions are presented in the following section.

- a. The analysis reveals a strong correlation between rapid changes in operating points (OPs) and the corresponding variations in velocity streamlines and velocity curl. For OP8, significant flow separation is observed within the runner flow passage. This separation diminishes at OP9.
- b. The pressure pulsation spectrum obtained via Fast Fourier Transform (FFT) analysis for the Reverse Pump Turbine (RPT) reveals a combined influence of Rotor-Stator Interaction (RSI) and operating condition-dependent local flow instabilities. Notably, operating point OP9 exhibits significantly higher-pressure pulsation amplitudes at both the Blade Passing Frequency (BPF) and local flow instability frequencies compared to OP8. Furthermore, the local flow instability frequencies are observed to be substantially higher at OP9.
- c. Fast Fourier Transform (FFT) analysis of pressure pulsations within the Reverse Pump Turbine (RPT) reveals significant differences between runners with and without splitter

blades. The analysis focuses on two key phenomena: Rotor-Stator Interaction (RSI) and local flow instabilities. Both RSI and local flow instabilities exhibit high pressure pulsation amplitudes. This suggests significant pressure fluctuations within the turbine due to unsteady flow interactions. Introducing wrap angle with splitter blades leads to a marked reduction in the pressure pulsation amplitudes for both RSI and local flow instabilities. This indicates improved flow stability and reduced pressure fluctuations within the turbine.

- d. The wrap angle with the splitter blade further influences the pressure pulsation amplitudes. The bigger wrap angle with splitter blade (WA2) demonstrates the lowest amplitude, which gradually increases as the blade wrap angle with splitter blades is reduced. This trend suggests that bigger wrap angle with splitter blades promote more effective flow stabilization. These findings are corroborated by the previously analyzed velocity streamlines and velocity curl figures. The runner without splitter blades exhibits a higher prevalence of backflow cells and vortices compared to runners with wrap angle with splitter blades. Additionally, these flow instabilities become more pronounced as the wrap angle with splitter blade decreases.

## Chapter6 Recommendations

### **1. Explore a wider range of operating points (OPs):**

The current study focused on 2 OPs. Consider expanding the analysis to include additional points, particularly those between OP8 and OP9 where significant changes in flow behavior were observed. This will provide a more comprehensive understanding of how flow instabilities evolve across the operating range.

### **2. Investigate the impact of GVO on flow instabilities:**

The study used a large GVO (34mm). Analyze how different GVO settings affect flow instabilities and their interaction with wrap angle with splitter blade configurations. This will provide insights into optimizing RPT operation for various flow conditions.

### **3. Evaluate unsteady forces and moments:**

Complement the flow analysis by calculating the unsteady forces and moments acting on the runner. This will provide insights into potential imbalances and vibrations experienced by the turbine due to flow instabilities.

### **4. Explore different wrap angle with splitter blade designs:**

The study focused on wrap angle with splitter blade. Consider investigating variations in other design parameters like blade length, thickness, and number of blades. This will help identify the optimal wrap angle with splitter blade design for minimizing flow instabilities across a wider operating range.

## References

1. Bachus, L. and A. Custodio, *Know and understand centrifugal pumps*. 2003: Elsevier.
2. <Pumped storage machines.pdf>.
3. <11\_06\_Broschuere-Pumped-storage\_einzeln.pdf>.
4. Britannica, E., *turbine summary*, in *Britannica*, E. Britannica, Editor. 2nd , May ,2020.
5. Tao, R., X. Song, and C. Ye, *Pumped Storage Technology, Reversible Pump Turbines and Their Importance in Power Grids*. Water, 2022. **14**(21): p. 3569.
6. Global, V., *Hydropower plant plus energy storage*.
7. Yu, H., et al., *Numerical investigation of splitter blades on the performance of a forward-curved impeller used in a pump as turbine*. Ocean Engineering, 2023. **281**: p. 114721.
8. *CHAPTER 5 - Hydraulic turbines, in Turbines, Generators and Associated Plant (Third Edition)*. 1991, Pergamon: Oxford. p. 422-445.
9. Binama, M., et al., *Flow instability transferability characteristics within a reversible pump turbine (RPT) under large guide vane opening (GVO)*. Renewable Energy, 2021. **179**: p. 285-307.
10. Li, G., et al., *Effects of the Splitter Blade on the Performance of a Pump-Turbine in Pump Mode*. Mathematical Problems in Engineering, 2018.
11. Olimstad, G., T. Nielsen, and B. Børresen, *Dependency on Runner Geometry for Reversible-Pump Turbine Characteristics in Turbine Mode of Operation*. Journal of Fluids Engineering, 2012. **134**(12).
12. Gui, Z., et al., *Analysis of the Energy Loss Mechanism of Pump-Turbines with Splitter Blades under Different Characteristic Heads*. Water, 2023. **15**(15): p. 2776.
13. Yuan, Y. and S. Yuan, *Analyzing the effects of splitter blade on the performance characteristics for a high-speed centrifugal pump*. Advances in Mechanical Engineering, 2017. **9**: p. 168781401774525.
14. Linsheng, X., et al., *Evolution of flow structures and pressure fluctuations in the S-shaped region of a pump-turbine*. Journal of Hydraulic Research, 2018. **57**: p. 1-15.

15. Binama, M., et al., *Investigation on reversible pump turbine flow structures and associated pressure field characteristics under different guide vane openings*. Science China Technological Sciences, 2019. **62**(11): p. 2052-2074.
16. Lenarcic, M. and A. Gehrler, *A theoretical, numerical and experimental analysis of S-shape instabilities in reversible pump-turbines: Resultant strategies for improving operational stability*. IOP Conference Series: Earth and Environmental Science, 2019. **240**: p. 032023.
17. Dong, G., et al., *The Splitter Blade Pump–Turbine in Pump Mode: The Hump Characteristic and Hysteresis Effect Flow Mechanism*. Processes, 2024. **12**: p. 324.
18. Yasa, T., S. Lavagnoli, and G. Paniagua, *Impact of a Multi-Splitter Vane Configuration on the Losses in a 1.5 Turbine Stage*. 2011.
19. Lai, X.-D., et al., *Experimental investigation of flows inside draft tube of a high-head pump-turbine*. Renewable Energy, 2019. **133**: p. 731-742.
20. Xiao, W., et al., *Pressure pulsation of pump turbine at runaway condition based on Hilbert Huang transform*. Frontiers in Energy Research, 2024. **12**.
21. Li, D., et al., *Optimization of blade high-pressure edge to reduce pressure fluctuations in pump-turbine hump region*. Renewable Energy, 2022. **181**: p. 24-38.
22. Mao, X., et al., *Investigation on optimization of self-adaptive closure law for load rejection to a reversible pump turbine based on CFD*. Journal of Cleaner Production, 2021. **283**: p. 124739.
23. Ren, S., et al., *The Influence of Hydraulic Characteristics on Structural Performance in a Pump-Turbine under No-Load Conditions*. Processes, 2023. **11**(12): p. 3422.
24. Wang, W., et al., *Transient simulation on closure of wicket gates in a high-head Francis-type reversible turbine operating in pump mode*. Renewable Energy, 2019. **145**.
25. Hu, J., et al., *Transition of amplitude–frequency characteristic in rotor–stator interaction of a pump-turbine with splitter blades*. Renewable Energy, 2023. **205**: p. 663-677.
26. Wang, W., et al., *Transient simulation on closure of wicket gates in a high-head Francis-type reversible turbine operating in pump mode*. Renewable Energy, 2020. **145**: p. 1817-1830.
27. Zhang, Y. and Y. Wu, *A review of rotating stall in reversible pump turbine*. Proceedings of the Institution of Mechanical Engineers, Part C: Journal of Mechanical Engineering Science, 2017. **231**: p. 1181–1204.
28. Meng, L., *Study on the Pressure Pulsation inside Runner with Splitter Blades in Ultra-High Head Turbine*. Vol. 22. 2014.

29. Deyou, L., et al., *Unsteady simulation and analysis for hump characteristics of a pump turbine model*. Renewable Energy, 2015. **77**: p. 32-42.
30. Fu, X., et al., *Mechanism of low frequency high amplitude pressure fluctuation in a pump-turbine during the load rejection process*. Journal of Hydraulic Research, 2021. **59**(2): p. 280-297.
31. Hu, D., et al., *Distribution Features of Flow Patterns and Pressure Pulsations of Pump-Turbine in Five Operating Modes on the Four-Quadrant Plane*. Frontiers in Energy Research, 2022. **10**.
32. Fu, X., et al., *Dynamic characteristics of a running away pump-turbine with large head variation: 1D + 3D coupled simulation*. Engineering Applications of Computational Fluid Mechanics, 2023. **17**.
33. Hasmatuchi, V., et al., *Experimental investigation of a pump-turbine at off-design operating conditions*. 2009.
34. Qin, Y., et al., *Comprehensive hydraulic performance improvement in a pump-turbine: An experimental investigation*. Energy, 2023. **284**: p. 128550.
35. Liu, D.-m., W.-l. Xu, and Y.-z. Zhao, *Experimental study of the flow field of a high head model pump turbine based on PIV technique*. Journal of Hydrodynamics, 2021. **33**: p. 1045-1055.
36. Deng, W., et al., *Laser Doppler Velocimetry Test of Flow Characteristics in Draft Tube of Model Pump Turbine*. Processes, 2022. **10**: p. 1323.
37. Han, Y. and L. Tan, *Experimental investigation on spatial-temporal evolution of tip leakage cavitation in a mixed flow pump with tip clearance*. International Journal of Multiphase Flow, 2023. **164**: p. 104445.
38. Zhang, X., et al., *Experimental and Numerical Analysis of Performance Discontinuity of a Pump-Turbine under Pumping Mode*. IOP Conference Series: Earth and Environmental Science, 2016. **49**(4): p. 042003.
39. Ji, L., et al., *Experimental and Numerical Simulation Study on the Flow Characteristics of the Draft Tube in Francis Turbine*. Machines, 2022. **10**(4): p. 230.
40. Vagnoni, E., et al., *Interaction of a rotating two-phase flow with the pressure and torque stability of a reversible pump-turbine operating in condenser mode*. International Journal of Multiphase Flow, 2018. **111**.
41. Horlock, J.H. and J.D. Denton, *A Review of Some Early Design Practice Using Computational Fluid Dynamics and a Current Perspective*. Journal of Turbomachinery, 2005. **127**(1): p. 5-13.
42. Li, G., et al., *Numerical Investigation of the Transient Flow and Frequency Characteristic in a Centrifugal Pump with Splitter Blades*. Journal of Thermal Science, 2021. **30**(2): p. 562-573.

43. Ješe, U., R. Fortes Patella, and M. Dular, *Numerical Study of Pump-Turbine Instabilities Under Pumping Mode Off-Design Conditions*. 2015.
44. Guo, X., et al., *Numerical and experimental investigations on the cavitation characteristics of a high-speed centrifugal pump with a splitter-blade inducer*. *Journal of Mechanical Science and Technology*, 2015. **29**(1): p. 259-267.
45. Yan, J., U. Seidel, and J. Koutnik, *Numerical simulation of hydrodynamics in a pump-turbine at off-design operating conditions in turbine mode*. *IOP Conference Series: Earth and Environmental Science*, 2012. **15**: p. 2041.
46. Braun, O., J.-L. Kueny, and F. Avellan, *Numerical Analysis of Flow Phenomena Related to the Unstable Energy-Discharge Characteristic of a Pump-Turbine in Pump Mode*. 2005.
47. Zhu, B., et al., *Optimization design of a reversible pump–turbine runner with high efficiency and stability*. *Renewable Energy*, 2015. **81**: p. 366-376.
48. analizis, c.s. *Methods for Grid Generation in CFD Simulations*. 2021 [21 July 2023]; Available from: <https://resources.system-analysis.cadence.com/blog/msa2021-methods-for-grid-generation-in-cfd-simulations>.